Western Graduate&PostdoctoralStudies

Western University
Scholarship@Western

Electronic Thesis and Dissertation Repository

10-13-2020 2:30 PM

Reactive oxygen species damage and consequences for mitochondrial function in the hibernating thirteen-lined ground squirrel, Ictidomys tridecemlineatus

Brynne Duffy, *The University of Western Ontario*

Supervisor: Staples, James F., *The University of Western Ontario*

A thesis submitted in partial fulfillment of the requirements for the Master of Science degree in Biology

© Brynne Duffy 2020

Follow this and additional works at: https://ir.lib.uwo.ca/etd

Part of the Biology Commons, and the Physiology Commons

Recommended Citation

Duffy, Brynne, "Reactive oxygen species damage and consequences for mitochondrial function in the hibernating thirteen-lined ground squirrel, Ictidomys tridecemlineatus" (2020). *Electronic Thesis and Dissertation Repository*. 7467.
https://ir.lib.uwo.ca/etd/7467

This Dissertation/Thesis is brought to you for free and open access by Scholarship@Western. It has been accepted for inclusion in Electronic Thesis and Dissertation Repository by an authorized administrator of Scholarship@Western. For more information, please contact wlswadmin@uwo.ca.

Abstract

Hibernators experience changes in blood flow, similar to ischemia-reperfusion injury, which may lead to oxidative damage. I hypothesized that suppression of mitochondrial metabolism during hibernation protects against such damage. I compared oxidative damage and antioxidant capacity in tissues and isolated liver mitochondria among summer, torpid, and interbout euthermic thirteen-lined ground squirrels (TLGS). I found less oxidative tissue damage during summer than hibernation, but no mitochondrial differences. I also compared metabolic activity of isolated mitochondria before and after five minutes of anoxia, followed by reoxygenation, among hibernation states and rats. Anoxia-reoxygenation decreased state-three respiration (ST3) in all groups, with rat mitochondria affected the most, and torpor TLGS mitochondria affected the least. With rotenone inhibition, ST3 was less affected by anoxia-reoxygenation, suggesting ETS complex-I is a source of ROS production. An exogenous antioxidant (ascorbate) mitigated changes in ST3. My findings suggest that metabolic suppression offers some protection against oxidative damage during hibernation.

Keywords

Anoxia-reoxygenation, high-resolution respirometry, ischemia, metabolic suppression, oxidative damage, reperfusion

Summary for Lay Audience

Maintaining body temperature is metabolically expensive for mammals experiencing cold winters. Hibernation is one strategy of avoiding this high metabolic cost. In addition to lowered metabolic rates (less than 10 % of summer values), hibernators experience low levels of oxygen, but many can tolerate these conditions. They are therefore often used to study the effects of ischemia (lack of blood flow)-reperfusion (regain of blood flow) experiments, such as what occurs in strokes. Suppressed metabolism during hibernation may be protective against low oxygen levels and temperatures.

Our species of interest, the thirteen-lined ground squirrel, cycles between states of very low and very high metabolic rate throughout the hibernation season. During torpor, ground squirrels drastically suppress metabolic rate, lower heart rate, and decrease body temperature. Torpor lasts for approximately two weeks, before arousal (in approximately 5 h). They remain at these high body temperatures and metabolic rate for approximately 8 hours, and then gradually drop back into torpor. During these metabolic fluctuations, blood flow and oxygen supply and demand fluctuate, possibly increasing reactive oxygen species (ROS, sometimes referred to as free radicals) production.

I compared markers of oxidative damage and antioxidant capacity (ability to detoxify ROS) among torpor, aroused, and summer ground squirrels to determine if hibernation protects squirrels against ROS damage. I also looked at the functional consequences of anoxia-reoxygenation at the mitochondrial respiration level, to determine how mitochondrial respiration was affected by oxygen fluctuation.

I found that summer ground squirrels had less oxidative damage than torpid and aroused animals, but antioxidant capacity did not differ, suggesting damage was due to higher ROS levels during hibernation. I also found that mitochondrial respiration rates were lower following anoxia-reoxygenation but were least affected in torpor when there is the most suppression of mitochondrial metabolism. Finally, I found that the addition of an antioxidant protected mitochondria against the effects of anoxia-reoxygenation. In summary, my findings indicate that metabolic suppression during torpor offers protection against changes in oxygen supply during hibernation.

Co-Authorship Statement

This thesis will be submitted in a modified form to the American Journal of Physiology, with Drs. Birgitte Jensen and James F. Staples as co-authors. I produced all data contained within the thesis. Dr. Jensen contributed to tissue sampling and mitochondrial isolation. I contributed to experimental concept and design, analysed data, and wrote the manuscript. Dr. Staples contributed to the experimental concept and design, as well as manuscript editing.

Acknowledgments

First and foremost, I need to thank my supervisor, Dr. Jim Staples, for his invaluable support and mentorship. Thank you for your encouragement, confidence, and trust. Thank you for motivating me to gain confidence in my work. I am very lucky and excited to keep working together for my PhD.

Secondly, I would like to thank the members of my advisory committee, Drs. Chris Guglielmo and Rob Cumming. Their advice has helped me to stay on track and prioritize. Thank you for your perspectives and experience.

Birgitte Jensen, thank you for your endless patience, especially when we were learning how to isolate ground squirrel mitochondria. Thank you for teaching me the magic of graphpad and goodnotes and most of all, thank you for your friendship.

Amalie Hutchinson, thank you for all your help with the school, and squirrels and all things 2019/20 threw our way. Thank you for your flexibility and constant positivity. I truly appreciate your encouragement and support.

Thank you Sharla Thompson for all the animal care support and advice. Thank you for your patience and diligence with everything squirrel related, and for finding us N95s this summer.

And of course, I need to thank my mom. Thank you for all of your guidance and reassurance.

Finally, thank you to my partner Tamsyn. The only one who could live with me, and still love me, during a pandemic that coincided with all of my thesis writing.

Table of Contents

Abstract i

Summary for Lay Audience ii

Co-Authorship Statement iii

Acknowledgments iv

Table of Contents v

List of Figures viii

List of Tables x

List of Appendices xi

List of Abbreviations xii

Chapter 1 1

1 Introduction 1

1.1 Endothermy 1

1.2 Hibernation 2

1.3 Thirteen lined ground squirrels 3

1.4 Metabolic Suppression in Hibernation 5

1.5 Blood Circulation 6

1.6 Ischemia-Reperfusion 7

1.7 Hypoxia and Ischemia-reperfusion tolerance 10

1.8 Mitochondrial Physiology 11

1.9 Reactive oxygen species 14

1.10 Reverse electron transport 15

1.11 ROS damage to cellular components 18

1.12 Antioxidant Defense 19

1.13 Objectives, hypotheses, predictions 22

Chapter 2 24

2 Methods 24
2.1 Experimental animals 24
2.2 Body temperature telemetry implants 24
2.3 Experimental groups 25
2.4 Tissue sampling 25
2.5 Mitochondrial isolation 26
2.6 Lipid Peroxyl Content 27
2.7 Protein Carbonyl Content 28
2.8 DNA abasic sites 29
2.9 Total antioxidant capacity 31
2.10 Respirometry 31
2.11 Statistical analysis 33
Chapter 3 34
3 Results 34
3.1 Markers of oxidative damage in tissue 34
3.1.1 Lipid damage 34
3.1.2 Protein Damage 35
3.1.3 DNA damage 36
3.1.4 Total antioxidant capacity 37
3.2 Mitochondrial Respiration 39
3.2.1 Effect of anoxia reoxygenation on respiration 39
3.2.2 Effect of the antioxidant Ascorbate on anoxia-reoxygenated mitochondria 47
3.3 Markers of oxidative damage in isolated mitochondria 54
3.3.1 Freshly isolated mitochondria 54
3.3.2 Damage to mitochondria following anoxia-reoxygenation 55
Chapter 4 57

4 Discussion 57

4.1 The effect of hibernation state on markers of ROS damage and antioxidant capacity in tissue 58

4.1.1 4.1.1 Lipid peroxidation 58

4.1.2 Protein carbonylation 60

4.1.3 DNA damage 61

4.1.4 Total Antioxidant Capacity 62

4.2 Impacts of anoxia-reoxygenation on mitochondrial respiration, and mitigation by an exogenous antioxidant 63

4.2.1 The effect of anoxia-reoxygenation on mitochondrial performance 63

4.2.2 Effect of exogenous antioxidant on anoxia-reoxygenated mitochondria 66

4.3 Effect of anoxia-reoxygenation on markers of ROS damage to isolated mitochondria 67

4.3.1 Mitochondrial Protein Carbonylation 67

4.3.2 Mitochondrial Lipid Peroxidation 68

4.4 Oxidative damage and tolerance in hibernation 70

4.4.1 Oxidative damage during oxidative phosphorylation 70

4.4.2 Super-complexes 71

4.4.3 Ischemic Preconditioning 72

4.4.4 Antioxidants 72

4.5 Discussion summary 73

Chapter 5 74

5 Conclusions and future directions 74

References 76

Appendix 84

Curriculum Vitae 86

List of Figures

Figure 1. Mitochondrial effects of ischemia-reperfusion on ROS production. Dotted lines represent reduced activity.. 9

Figure 2. Mitochondrial bioenergetics and ROS production. NADH and succinate (derived from tricarboxylic acid cycle) donate electrons to complexes I and II of the electron transport system (ETS). 13

Figure 3. Effects of rotenone inhibition on “forward” (A), and “reverse” (B) electron transport. 17

Figure 4. Systems for protection against reactive oxygen species.. 21

Figure 5. Markers of reactive oxygen species damage to lipids (A) and proteins (B) in 8 tissues of torpid, IBE and summer ground squirrels.. 36

Figure 6. Apurinic/apyrimidinic (AP) sites of DNA damage in heart, brown adipose tissue, liver and gastrocnemius muscle of torpid, IBE and summer ground squirrels. 37

Figure 7. Total antioxidant capacity (Trolox equivalent capacity) in 8 tissues of torpid, IBE and summer ground squirrels,. 38

Figure 8. The effect of anoxia-reoxygenation on maximal respiration (state 3) rates in isolated liver mitochondria of IBE, torpor, summer TLGS and rat.....41

Figure 9. The effect of anoxia-reoxygenation on leak respiration (state 4) rates in isolated liver mitochondria of IBE, torpor, summer TLGS and rat. 45

Figure 10. Effect of ascorbate maximal respiration (State 3) rates after anoxia-reoxygenation in isolated liver mitochondria of IBE and torpor ground squirrels.. 49

Figure 11. Effect of ascorbate on leak respiration (state 4) rates after anoxia-reoxygenation in isolated liver mitochondria of IBE and torpor ground squirrels.....52

Figure 12. Markers of reactive oxygen species damage to proteins (A) and lipids (B) in freshly isolated liver mitochondria from torpor, IBE and summer ground squirrels. 54

Figure 13. The effect of anoxia-reoxygenation on oxidative damage to mitochondrial proteins and lipids. 56

List of Tables

Table 1. Estimated marginal means (EMM) of post anoxia reoxygenation ST3 respiration..42

Table 2. Estimated marginal means (EMM) of post anoxia reoxygenation ST4 respiration..46

Table 3. Estimated marginal means (EMM) of post anoxia reoxygenation ST3 respiration with ascorbate……..50

Table 4. Estimated marginal means (EMM) of post anoxia reoxygenation ST4 respiration with ascorbate……..53

List of Appendices

Appendix 1: Animal use ethics approval.....84

Appendix 2: Interaction plot of the respiratory control ratio (RCR) of liver mitochondria before (pre) and post anoxia-reoxygenation. 85

List of Abbreviations

ADP	adenosine 5'-disphosphate
ATP	adenosine triphosphate
BAT	brown adipose tissue
BHT	butylated hydroxytoluene
BSA	bovine serum albumin
CoQ	coenzyme Q
ETS	electron transport system
$FADH_2$	flavin adenine dinucleotide, reduced
GSH	reduced glutathione
GSSH	oxidized glutathione
IBE	interbout euthermia
IMM	inner mitochondrial membrane
IMS	intermembrane space
MnSOD	magnesium superoxide dismutase
MTP	mitochondrial permeability transition pore
NAD^+	nicotinamide adenine dinucleotide
NADH	Nicotinamide adenine dinucleotide, reduced
$O_2\cdot$	Superoxide
RET	Reverse electron transport

RCR	respiratory control ratio
ROS	reactive oxygen species
S	summer
ST3	state 3 respiration
ST4	state 4 respiration
T	torpor
T_a	ambient temperature
T_b	body temperature
TCA	tricarboxylic acid
TLGS	thirteen-lined ground squirrels
TNZ	thermal neutral zone
UCP	uncoupling protein
$UQ^{\bullet-}$	ubiquinone

Chapter 1

1 Introduction

1.1 Endothermy

Endothermy and ectothermy are two thermoregulatory patterns found in animals. In ectotherms, body temperature varies with ambient temperature. Some ectotherms can regulate body temperature using behavioural thermoregulation, which alters heat exchange with the environment. In addition to behaviour, endotherms use physiological mechanisms to alter heat exchange. Endotherms actively regulate body temperature using the metabolic production of heat, thereby maintaining fairly constant body temperature despite changes in ambient temperature. Due to the metabolic demands of thermoregulation, endotherms often have resting metabolic rates 5-15 times higher than ectotherms of a similar size (47). For example, a mouse (*Mus musculus*) and netted dragon (*Amphibolurus nuchalis*), an endotherm and ectotherm respectively of similar mass and body temperature, mice have basal metabolic rates 8-fold higher (35). Mitochondrial membrane surface areas from metabolically active tissues are greater in the endotherm, reflecting these differences in whole-animal metabolism (35).

Body size also influences energy expenditure, as body size is a determinant of basal metabolic rate (70). In most cases, total basal expenditures are believed to be proportional to the body mass raised to the exponent 0.75 (70). This allometric relationship applies to both endotherms and ectotherms and, although the underlying mechanism remains debated, the higher surface area to volume ratio in smaller animals is likely influential. At low ambient temperatures, small endotherms experience very high metabolic demands, as they must endogenously increase heat production to thermoregulate. Some endotherms migrate to avoid such challenging environmental conditions while others adjust their energy metabolism.

To survive the challenge of low ambient temperatures, endotherms can use two energetic strategies. First, an animal can remain active throughout the winter, increasing metabolic heat production with an increased metabolic rate. These animals minimize heat

loss to the environment by increasing physical insulation in the form of body fat, fur, or feathers. These animals also must ensure an adequate supply of food energy to fuel high metabolic rates. Typically, small endotherms cache food, whereas larger endotherms rely more on increasing fat stores (70). A second strategy used by some endotherms is to reduce energy demand by decreasing metabolic rate (and, consequently, body temperature), as in daily torpor or hibernation.

1.2 Hibernation

Hibernation can be defined as a metabolic suppression to less than 10 % of resting values for several days, with corresponding decreases in body temperature (99). Compared to hibernation, daily torpor describes periods of reduced metabolic rate to levels not below 26 % of resting values for less than 24 hours, with a decrease in body temperature, not below 11 °C (99).

While hibernation is often associated with low winter temperatures, metabolic suppression and decreased body temperature can occur in some species during other challenging environmental conditions. For example, during estivation, the Madagascan fat-tailed dwarf lemur, *Cheirogaleus medius*, reduces metabolism and body temperature for several months (26). Estivation has physiological patterns almost indistinguishable from winter hibernation but occurs under warm and dry conditions, typically with decreased food availability.

Two classifications of hibernation are facultative and obligate. Facultative hibernation only occurs in response to challenging environmental conditions, such as reduced food availability or low temperatures. For example, the facultative hibernator Syrian hamster, *Mesocricetus auratus*, does not appear to have an endogenous hibernation rhythm but instead can be induced into hibernation at any time of the year by acclimatization to short photoperiod and low ambient temperature (19). In field conditions, facultative hibernators such as the black-footed prairie dog (*Cynomus ludovicianus*) vary in whether they hibernate seasonally with geographic areas and environmental conditions (59).

In obligate hibernation, an endogenous circannual rhythm seems to regulate hibernation, which occurs every year, regardless of environmental conditions. The golden-mantled ground squirrel, *Callospermophilus lateralis,* demonstrates a strict endogenous rhythm, with yearly cycles of metabolic suppression and body temperature irrespective of ambient temperature or photoperiod (86). Our species of interest, the thirteen lined ground squirrel (TLGS), *Ictidomys tridecemlineatus*, is considered an obligate hibernator as many physiological processes begin before torpor entrance. For example, the TLGS increases thoracic brown adipose tissue deposits from spring to autumn before any decrease in ambient temperatures (64). However, this species was only assumed to be an obligate hibernator until a recent study showed that TLGS housed at constant temperature (either 5 °C, 16 °C or 25 °C) and photoperiod (12:12/ L:D) for an entire year, all began hibernating in autumn and stopped hibernating in spring (MacCannell and Staples, in revision, J. Therm. Biol.).

Hibernation, which is predominantly restricted to mammals, is found in all three mammalian groups: Monotremata (Prototheria), Marsupialia (Metatheria) and Placentalia (Eutheria) (42, 90). While several diverse bird species, including *Dacelo novaeguineae* (24), *Amazilia versicolor* (5) and even an owl species, *Otus senegalensis* (94) can engage in daily torpor, only one bird species, the common poorwill, *Phalaenoptilus nuttalli*, has been documented to undergo prolonged torpor, possibly with active metabolic regulation that resembles hibernation in mammals (109). The occurrence of hibernation across at least 11 mammalian orders suggests that non-hibernators diverged recently from presumptive hibernating ancestors (90). For example, non-hibernating rodents from tribes Funambulini and Protoxerinin, diverged recently from the tribe Marmontini, which include the hibernating ground squirrels (93). Thirteen lined ground squirrels are one of the best-studied hibernating ground squirrels.

1.3 Thirteen lined ground squirrels

As briefly explained above, thirteen lined ground squirrels (TLGS) are obligate hibernators that inhabit central North America in prairie grassland environments. Adults have a body mass of between 150-300 g and have distinctive dorsal markings of alternating continuous and dotted lines. The ground squirrels used in this study originate

from Carman Manitoba (49° 30'N, 98° 01'W), where they live in extensive burrows that delve beneath the frost line. Early field studies report patterns of hibernation as far north as Manitoba (26), and as far south as Texas (68), with hibernation seasons starting earlier and lasting longer in Manitoba than in the southern populations such as Texas, coinciding with the winter season duration.

Like other hibernators, the TLGS cycle between two distinct states during the hibernation season: torpor and interbout euthermia (IBE). During torpor, TLGS decrease body temperature from euthermic values (35-38 °C) to torpid values (4-8 °C) (56), metabolic rate to less than 5 % of euthermic values (72), and heart rate from 350-400 to as low as two beats per minute (62). This torpid period lasts for approximately 12 days when it is interrupted by arousal, which brings the animal to interbout euthermia (IBE).

During arousal, non-shivering thermogenesis rewarms the body with endogenous heat produced by brown adipose tissue mitochondrial respiration in which substrate oxidation is uncoupled from ATP synthesis. Shivering thermogenesis by skeletal muscle occurs once the body warms to approximately 15 °C. During arousal, metabolic rate (22) and heart rate (62) increase before any rise in body temperature. However, the mechanism that triggers arousal is still unknown.

In IBE, animals maintain euthermic body temperatures and high, steady metabolic rates for approximately 8 hours, after which TLGS re-enter torpor over 12 hours. This cycle continues for the five months of hibernation season, with torpor bouts initially increasing in duration as the season progresses, then shortening as spring approaches. Males tend to terminate hibernation slightly before the females.

From mid-spring to early autumn, TLGS maintain euthermic conditions similar to those reached in IBE. Mating occurs shortly after females emerge from hibernation, with an average gestation period of 28 days, followed by a nursing period of approximately 30 days until pups are weaned (104). For adults, the rest of the non-hibernating season is devoted to weight gain, predominately through stored adipose tissue. Under laboratory conditions, both sexes gain weight rapidly through late June, July and early August (4). Reproductive females take longer to gain weight; thus, they enter hibernation later than

males and reduce activity shortly after the mating season (104). As early as 1930, field and laboratory observations found that TLGS can gain enough weight in three weeks to survive six months of hibernation (105). TLGS body mass increases by 30% from active summer to the beginning of hibernation (92). Thoracic brown adipose tissue (BAT) depots increase more than two-fold in volume from spring through autumn, even when animals are housed at constant 22 °C and subsequent cold exposure (5 °C) enlarges the thoracic BAT further by 40 % (63).

1.4 Metabolic Suppression in Hibernation

The reduction in metabolic rate during entrance into torpor results from three factors: passive thermal effects, decreased thermogenic metabolism, and active metabolic suppression. During torpor entrance, the thermoregulatory set-point progressively decreases, as the establishment of a new lower range of thermal neutral zone occurs, resulting in decreased thermogenic metabolism from BAT, shivering, and a subsequent fall in body temperature.

Cooling also reduces the metabolic rate by passive thermal effects. This fall is also reflected in the Q_{10} values that describes the relationship between body temperature and VO_2 (oxygen consumption, a proxy measurement of metabolic rate). Q_{10} values between two and three suggest that passive thermal effects are the primary contributor to reducing metabolism. A decrease in 10 °C will reduce the rate of most biological processes by two to three-fold. This so-called “Arrhenius effect” can account for part of the metabolic suppression seen in torpor. However, Q_{10} values of metabolic rates between the euthermic and torpid states tend to be greater than three, suggesting that a decrease in tissue temperature alone cannot explain the reduction in metabolic rate observed in hibernators (95). For example, during entrance into torpor of the golden mantled ground squirrel, the Q_{10} of metabolic rate between euthermia and deep torpor is 3.5 (95). Moreover, anesthetized non-hibernating ground squirrels cooled exogenously had metabolic rates 15-fold higher than torpid animals at the same body temperature, suggesting that cooling the body cannot account for the total decrease in metabolic rate observed in hibernation on its own (107).

The third contribution to metabolic rate reduction during entrance to torpor is the active suppression of metabolism in non-thermogenic tissues. A reduction in metabolism before any change in body temperature indicates the contribution of an active and regulated mechanism that conserves energy during torpor. Such active metabolic suppression is reflected by significant decreases in isolated liver mitochondrial metabolism. In torpor, maximum mitochondrial metabolic rate is suppressed 70 % compared to IBE in the liver (72), 60 % in brown adipose tissue (69), and 30 % in skeletal muscle (11) and cardiac muscle (12). For liver mitochondria, this suppression is complete before body temperature falls below 30 °C during entrance into torpor (99).

The degree of mitochondrial metabolic suppression depends on the oxidative substrate(s) and measurement temperature. In liver mitochondria, suppression of respiration is greatest in torpor when succinate is oxidized (72). Animals sampled in torpor and IBE have body temperatures near 5 °C and 37 °C, respectively, but it is best to compare respiration between hibernation states at the same temperature to remove any temperature effects. In liver mitochondria isolated from TLGS, the greatest difference (70 %) in maximal respiration rates between torpor and IBE occurs when respiration is measured *in vitro* at 37 °C. When measured at 25 °C, this difference (65 %) is lessened but still significant. When measured at 10 °C, however, respiration rates do not differ between torpor and IBE (11).

1.5 Blood Circulation

Along with changes in whole-animal oxygen consumption rates and mitochondrial metabolism, hibernation is characterized by drastic reduction in heart rate, blood pressure, and blood flow relative to euthermia. Heart rate increases from 2.2 to 5 beats per minute during arousal from torpor to IBE before there is any detectable change in body temperature and continues to increase to as high as 200-300 beats per minute (62). Blood pressure also increases from 60/30 mm Hg during torpor to 140/100 mm Hg during arousal (62). Despite these drastic changes, electrocardiograms of TLGS hearts still show strong QRS wave peaks, with broad spacing, suggesting strong, distinct heartbeats that further contribute to rapid changes in blood pressure and blood flow (45). Platelet abundance is lower during hibernation than summer conditions, reducing

possible slowing or blockage of blood flow (10). Blood clotting time increases during arousal, suggesting that restoration of blood flow to tissues during arousal is not impeded by clotting factors as it is in the summer euthermic phenotype (10).

1.6 Ischemia-Reperfusion

Due to the rapid and large changes in heart rate, blood pressure, and blood flow, each arousal can be considered similar to an ischemia-reperfusion event, where hypoperfused (similar to ischemia), hypoxic, and cold tissues are rapidly reoxygenated and warmed by increased blood delivery (reperfusion) (55). Ischemia-reperfusion injury represents the sum of damage invoked by both states—it seems likely that ischemia causes primary injury and is exacerbated by reperfusion.

Ischemia (Figure 1A) denotes a lack of blood flow to tissues. During ischemia, due to the lack of O_2 delivery, anaerobic metabolism typically prevails, resulting in decreased cellular pH. Despite activation of glycolysis, cellular ATP typically decreases, potentially leading to the opening of the mitochondrial permeability transition pore (MPT), which dissipates mitochondrial membrane potential and further impairs ATP production (Figure 1A). Impaired ATP production consequently results in dysfunctional ATPase-dependent ion transport mechanisms, contributing to increased intracellular and mitochondrial calcium levels, cell swelling and rupture, and cell death.

Reperfusion (Figure 1B) restores the delivery of oxygen and substrates required for oxidative phosphorylation but may also have damaging consequences. This reperfusion injury is thought to be caused by the generation of mitochondrial reactive oxygen species (ROS) fueled by the reintroduction of molecular oxygen when blood flow is re-established. Damage by ROS may cause the opening of the MTP, endothelial dysfunction, and pronounced inflammatory responses (51). Reperfusion can have broader effects at the tissue level, damaging blood vessels resulting in drastic changes in blood flow or causing rewarming injury to distant tissues (81).

The duration of ischemic periods seems to affect the magnitude of ischemia-reperfusion injury. Short periods have been termed “ischemic preconditioning” and

appear to mitigate tissue damage from subsequent, longer periods. For example, in humans, exposure of the heart to short (5 min) bouts of ischemia-reperfusion before prolonged (40 min) reductions in coronary blood flow, resulted in infarct-sparing effects (76). Ischemic preconditioning indicates that the response to ischemia is bimodal, with more extended periods of ischemia inducing cell dysfunction and cell death exacerbated by reperfusion. In contrast, short cycles of ischemia are protective, rendering tissues resistant to the deleterious effects of prolonged ischemia followed by reperfusion (51).

Changes in blood flow during arousal in TLGS may result in damage similar to ischemia-reperfusion injury studied in other mammals. Each torpor period (~12 days) can be considered prolonged ischemia by human standards and may result in extensive ischemia-reperfusion damage during arousal. However, TLGS undergo these reperfusion events 10-20 times per hibernation season during arousal cycles and likely have adapted protective mechanisms against ischemia-reperfusion injury and oxidative damage.

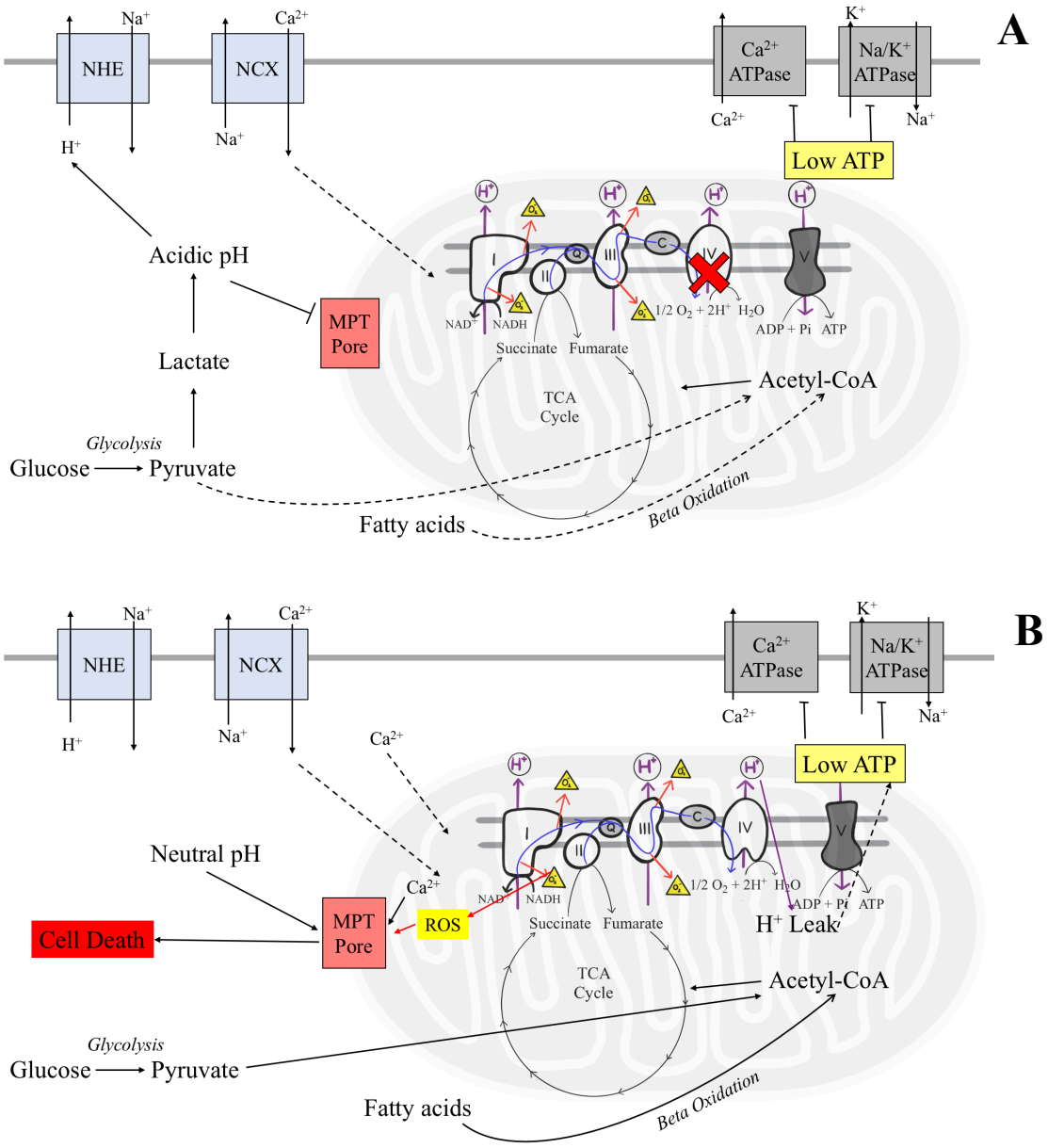

Figure 1. Mitochondrial effects of ischemia-reperfusion on ROS production. Dotted lines represent reduced activity. During ischemia (A), lack of O_2 inhibits oxidative phosphorylation diverting the glycolytic end product pyruvate, to lactate, resulting in cellular acidification. Disposal of acid via the Na^+/H^+ exchanger (NHE) brings Na^+ into the cytosol. This Na^+ is exported via the Na^+/Ca^{2+} exchanger (NCX) causing cytosolic Ca^{2+} overload, which is exacerbated by low ATP inhibiting Ca^{2+} export by ATPases. Low mitochondrial membrane potential and acidic pH keep the mitochondrial permeability transition pore (MPT) closed. Reperfusion (B), rapid reestablishment of Ox-Phosphorylation and mitochondrial membrane potential results in mitochondrial Ca^{2+} overload and increased ROS generation. Together with normalization of pH, this triggers MPT opening, leading to cell death. ROS activates mitochondrial uncoupling (H^+ leak), which lowers ATP production. Modified from 106.

1.7 Hypoxia and Ischemia-reperfusion tolerance

Hypoxia tolerance in mammals and ectothermic vertebrates is associated with regulated metabolic suppression. Some examples include seals that reduce their metabolic rates during dives to keep within their aerobic limits (98). Another example are fossorial naked mole rats that live in chronically hypoxic burrows and can survive complete anoxia by reducing metabolic demand and switching to anaerobic metabolism (84). In addition to tolerating low body temperatures, the metabolic suppression seen in hibernators appears to contribute to hypoxia and ischemia-reperfusion tolerance (7). Moreover, increased concentrations and activity of antioxidants in the hibernation season relative to the summer may contribute to this tolerance (31).

Several TLGS tissues are known to tolerate ischemia-reperfusion. Mucosal tissue of the small intestine is damaged by ischemia-reperfusion in summer, non-hibernating TLGS, but not is not damaged in IBE (55). Similarly, livers isolated from TLGS in hibernation retain cellular function and mitochondrial integrity better than in summer TLGS or rats after 72 h of ischemia at low temperatures (4 °C) followed by warm (37 °C) reperfusion (60). Further, in both the summer and hibernation phenotypes, arctic ground squirrel neurons from the hippocampus, cortical and striatal brain regions, are protected from ischemia-reperfusion injury (32). Of the tissues mentioned above, the liver is studied extensively because of its high metabolic activity in euthermic conditions and drastic differences in mitochondrial metabolic activity between torpor and IBE.

In summary, it appears that hibernators engage physiological protective mechanisms that decrease oxidative damage that likely occurs during arousal. In TLGS, I predict that these protective measures are enhanced during the hibernation season and that conditions that mimic ischemia-reperfusion injury would be better mitigated and repaired during interbout euthermia than in the summer euthermic state.

1.8 Mitochondrial Physiology

Mitochondrial regulation is required to achieve the metabolic suppression found in hibernation. Mitochondria are bacterial-sized (volume 0.42 μm^3, 0.9 μm diameter in rat liver; 41) organelles bound by a double membrane that exist within most eukaryotic cells. In general, the total amount of mitochondrial membrane surface area is four times greater in mammalian tissue than in reptiles, because mammals have relatively larger tissues with a greater proportion of cell volume occupied by mitochondria, and to a lesser extent higher internal mitochondrial membrane surface area density (37). Mitochondria synthesize the vast majority of ATP in cells through oxidative phosphorylation but are also involved in cell signaling, apoptosis regulation and ROS production.

Oxidative phosphorylation consists of a series of redox reactions, linked by increasingly electronegative electron acceptors along the electron transport system (ETS; Figure 2A). Six protein complexes comprise the ETS, located on and around the inner mitochondrial membrane. These include protein complexes I-IV, ubiquinone, and cytochrome c, each made up of several sub-proteins, including flavoproteins (64-73 kDa) and iron-sulfur proteins (~30 kDa). Electrons enter complex I (NADH-dehydrogenase) with the oxidation of NADH, or through complex II (succinate dehydrogenase) with the oxidation of succinate and $FADH_2$. In some tissues, electrons can also enter the ETS through the actions of other dehydrogenases including, electron transferring flavoprotein, ubiquinone oxidoreductase and glycerol-3-phosphate dehydrogenase.

During electron transfer from complexes I to IV, some of the free energy released from these sequential redox reactions' powers proton pumping through complexes I, III and IV from the mitochondrial matrix to the intermembrane space, against a proton gradient. This movement of protons establishes an electrochemical gradient known as the protonmotive force across the inner mitochondrial membrane. Oxygen acts as the final electron acceptor at complex IV, combining with protons and electrons to produce water in the mitochondrial matrix. Under high proton motive force and abundant ADP, protons flow passively through complex V (ATP synthase), powering ATP synthesis. (Figure 2A).

With saturating levels of ADP and electron-donating substrates, mitochondrial oxygen consumption coupled to ATP production can be measured to approximate the maximal physiological rate of oxygen consumption, or state three respiration (ST3). Even in the absence of ADP (and thus no ATP synthesis) some oxygen is consumed by the ETS because some protons move from the intermembrane space to the matrix across the inner mitochondrial membrane and bypass complex V; this is called leak respiration, or state four respiration (ST4). In intact mitochondria, the exact mechanism of this leak remains unknown, but damage to the inner mitochondrial membrane phospholipids can increase ST4.

In torpor, mitochondrial metabolism is suppressed, with lower ST3 respiration rates than in IBE and summer. For example, isolated TLGS liver mitochondria exhibit a 60 % reduction in pyruvate fueled ST3 respiration relative to IBE and summer values (65). ST4 rates are sometimes reported to be higher in torpor than in IBE and summer, suggesting leakier membranes in torpid conditions (45). These results suggest that mitochondrial oxidative capacity is reduced overall in torpor, and mitochondrial membranes may be more damaged in torpor than in IBE.

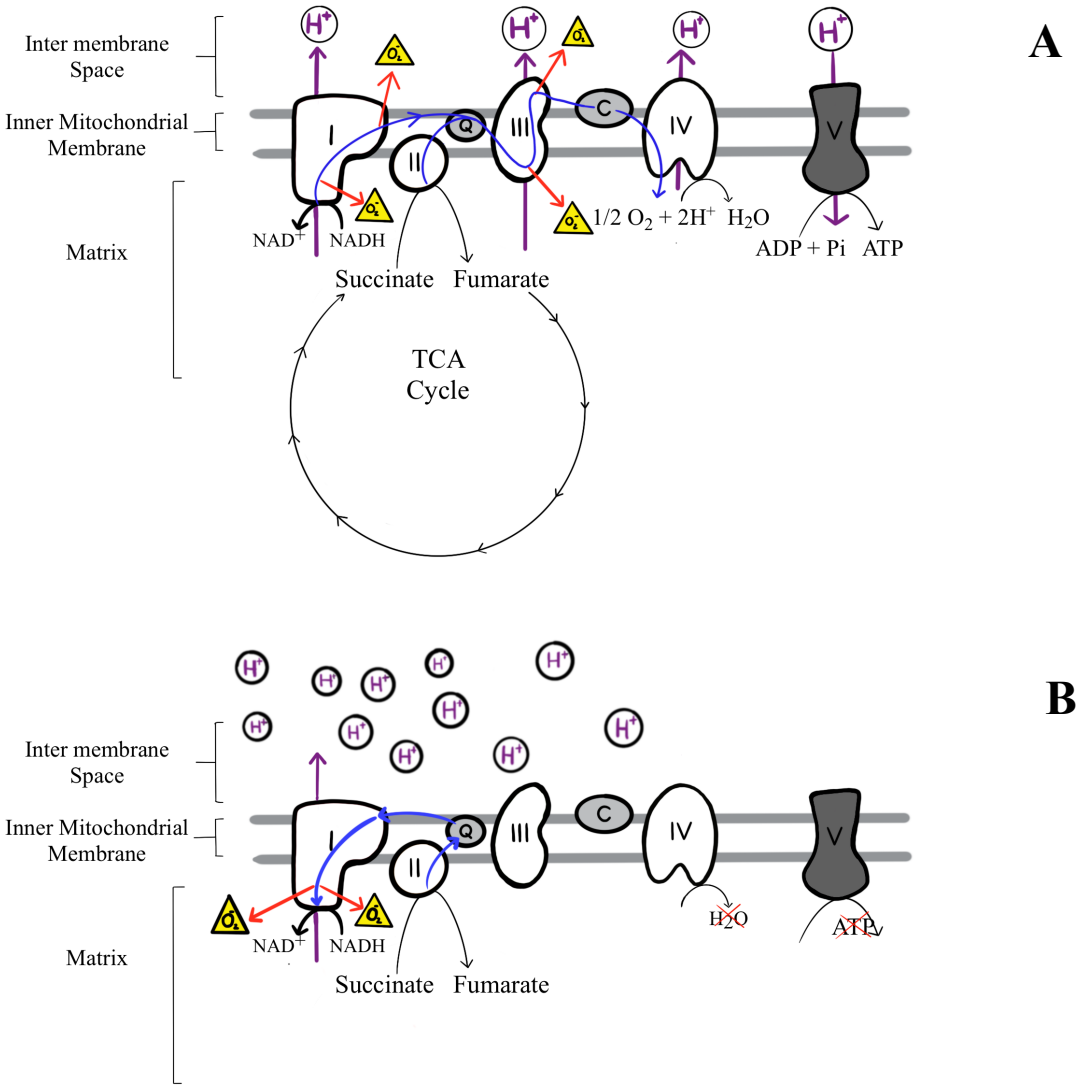

Figure 2. Mitochondrial bioenergetics and ROS production. NADH and succinate (derived from tricarboxylic acid cycle) donate electrons to complexes I and II of the electron transport system (ETS). Electrons are transferred through the ETS by a series of redox reactions. During forward electron transport (A), electrons are transferred from complex I to IV and lead to production of ATP. The final electron acceptor is oxygen. Highly reduced coenzyme Q pool and a high protonmotive force drives electrons in "reverse". During reverse electron transport (B), electrons are transferred from complex II and from succinate to ubiquinone towards complex I, and the final electron acceptor is NADH or oxygen (producing superoxide). RET often produces excess ROS from complex I, whereas forward electron transport produces ROS in both complex I and III. Energy released from redox reactions allows for proton (H^+) pumping from the matrix to intermembrane space. Modified from 66.

1.9 Reactive oxygen species

Oxidative damage can increase with a change in oxygen supply and demand, similar to the previously described arousal from torpor in TLGS. Mitochondria are the primary source of ROS production and can damage cellular components, including protein complexes, membrane lipids and nucleic acids. Even under normoxic conditions, a small portion of electrons passed through the ETS can partially reduce free O_2 to superoxide ($O_2^{\cdot-}$) which is further processed to generate other ROS species. There are 11 known sites of ROS production along the ETS, and their contribution to ROS generation depends on the bioenergetic condition of the cell (44). Most sites of ROS production occur in complexes I and III, in regions that interact with neighboring ETS complexes during electron transfer (44).

ROS production depends on many factors, including the proton motive force and available oxygen. Due to mass action effects, high proton motive force slows electron transfer through the ETS, which leads to increased electron leakage from ETS complexes and reduction of more O_2 to superoxide. For example, in complex III, the oxidation of ubiquinone ($UQ^{\bullet-}$) bound at the Q_p site depends on the passage of electrons by beta-cytochromes. This electron passage is slowed at high membrane potential and is therefore predicted to leak available electrons to O_2 creating ROS. Estimates of ROS production in respiring mitochondria vary from 0.1 % to as much as 4 % of total oxygen consumption, depending on the local oxygen concentration (77). Molecular oxygen is very electronegative, and so higher local O_2 concentrations more readily accept electrons than ETS proteins, further increasing the potential ROS production.

Superoxide ($O_2^{\bullet-}$) is the most abundant ROS initially produced by mitochondria when steps in the respiratory chain leak single electrons that react with O_2 to produce monovalent reductions (42). When there are drastic increases in O_2 concentrations, as during reperfusion following ischemia, more O_2 molecules are available to be reduced, and superoxide production increases. Within mitochondria, superoxide can damage proteins in the tricarboxylic acid (TCA) cycle, neighboring ETS proteins, and poly-unsaturated fatty acids, and also lead to the formation of more damaging ROS such as the hydroxyl radical ($HO^{\bullet}$) and hydroperoxyl ($HO_2^{\bullet}$). Superoxide is usually converted to

hydrogen peroxide (H_2O_2), a reaction catalyzed by superoxide dismutase (MnSOD in mitochondria and CuZnSOD in the cytoplasm).

Generation of H_2O_2 from $O_2^{\bullet}$ can also occur by non-enzymatic antioxidants such as ascorbate, thiols and flavonoids (Figure 4). Hydrogen peroxide has limited and selective reactivity that can make it an effective signaling molecule and is often part of a negative feedback loop that inactivates enzymatic antioxidants. Other forms of reactive oxygen species include the hydroxyl radical ($OH^{\bullet}$) produced by the reaction of metal ions with H_2O_2 or by UV-induced fission of the O-O bond in H_2O_2. The hydroxyl radical is the most reactive form of ROS, and once generated readily initiates lipid peroxidation, protein carbonylation, enzyme deactivation and DNA damage. (See section 1.11 for ROS damage to cellular components).

1.10 Reverse electron transport

Beyond the conditions leading to ROS production outlined above, recent research has highlighted another potentially important route, reverse electron transport (RET). Complex V (ATP synthase) is irreversible and is constrained to run "forward" (i.e. in the direction of ATP production) by a regenerated proton motive force higher than the thermodynamic equilibrium of the ETS, and the use of ATP by the cell. If there is inhibition of the respiratory chain, and continued supply of ATP to the mitochondria, or if Ca^{2+} depresses the proton motive force below the ATPase thermodynamic equilibrium, there is the potential for RET (Figure 2B) through complex V. RET may also be induced by a reverse flow of electrons from succinate or cytochrome c through complex I. These electrons can then transfer to O_2 to produce superoxide.

RET can drive superoxide production under conditions that create a highly reduced coenzyme Q pool and a high protonmotive force, which drives electrons "backward" through complex I, leading to a dramatic increase in ROS production. This pathway of ROS production leads to most oxidative damage from ischemia-reperfusion events, according to some studies. For example, complex I inhibitors such as rotenone decrease ROS generation in cultured myocytes during simulated ischemia (6, 20).

A proposed site of superoxide formation by RET is the flavin mononucleotide (FMN) subprotein of the complex I NADH-binding site. During RET, NADH reduces FMN to $FMNH^-$, which is then readily accessed by O_2 to form $O_2^{\bullet-}$. Rotenone inhibits complex I between the PSST and TYKY sub-proteins, located in the transmembrane portion of complex I (Figure 3). ROS production is higher during RET than when complex I is inhibited by rotenone as the large thermodynamic driving force for reverse electron movement through complex-I holds FMN/FMNH- at a more electronegative potential (-380 mV) than with the NAD^+/NADH pool (-335 mV) (89). This lessened ROS production likely occurs because the major ROS production site by RET on complex I is blocked from the electron flow by rotenone (77).

In summary, RET through complex I is a major source of ROS production, that can be prevented by rotenone. There is less ROS production when complex I is inhibited by rotenone, which suggests complex I is a major site of ROS production. However, ROS production occurs during “forward” electron transfer as well, so even with rotenone inhibition, it is likely that ROS can damage mitochondria during anoxia-reoxygenation.

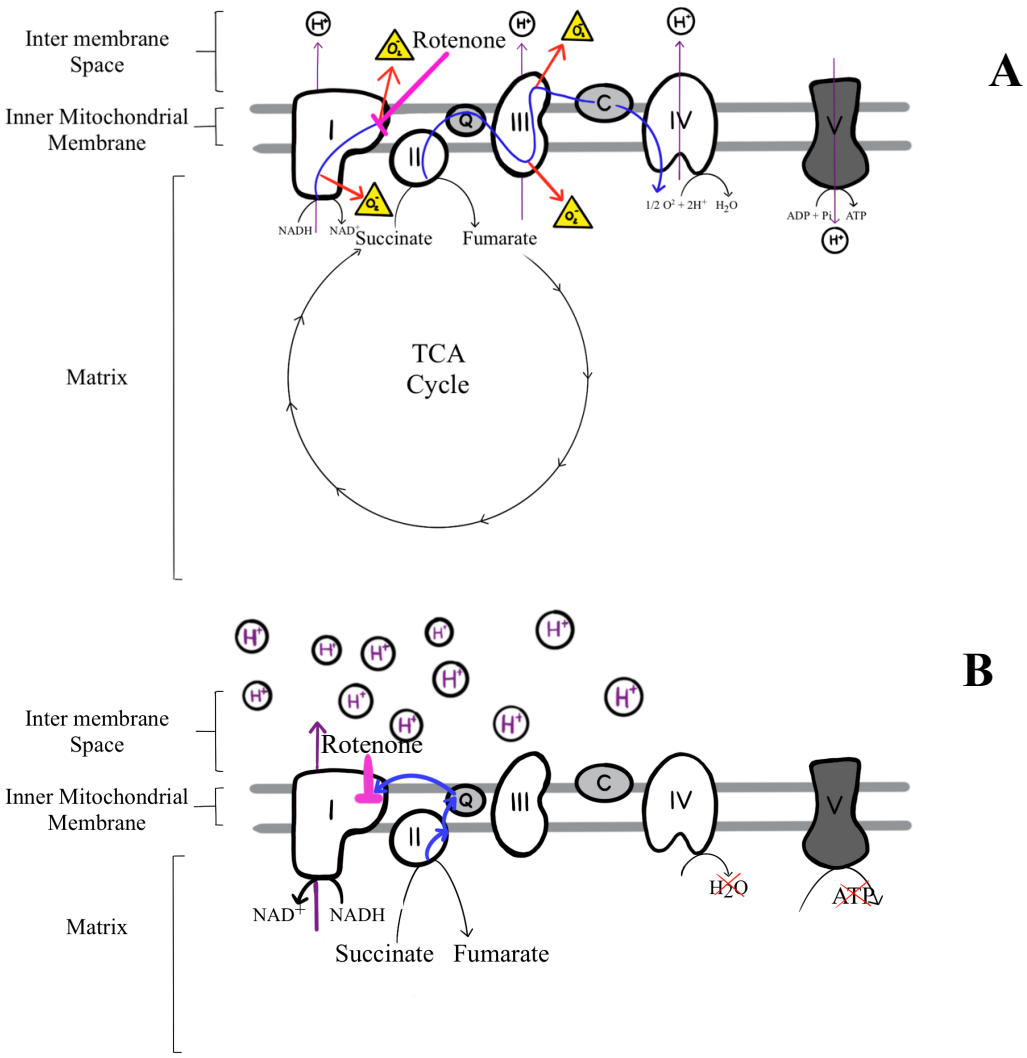

Figure 3. Effects of rotenone inhibition on "forward" (A), and "reverse" (B) electron transport. Rotenone inhibits complex I in forward electron transport (A) within the ETS by preventing electron transfer from PSST to TYKY subunits (named with respect to characteristic amino acid sequences) within the inner mitochondrial membrane. ROS production by complex I is upstream (on the NADH side) of the rotenone binding site, inhibiting ROS production through reverse electron transport (B). During reverse electron transport, the proton motive force is generated by succinate oxidation and drives electron transport in reverse. Modified from 66.

1.11 ROS damage to cellular components

Lipids are typically more susceptible to ROS damage than proteins or nucleic acids (44), and damage to them is easily detected. Further, lipid peroxidation in most biological membranes likely damages membrane-bound proteins as well. There are three steps in lipid oxidative damage: initiation, propagation and termination. During initiation, either ROS (usually $OH^{\bullet}$) is bound by addition to a lipid, or more commonly, a hydrogen atom is abstracted (removed by a radical) from a methane group of a phospholipid tail. In both cases, a carbon radical called a lipid peroxyl results. The presence of a double bond in lipids (a unit of unsaturation) weakens the C-H bond energy of the adjacent carbon atom, creating an allylic hydrogen that is more easily oxidized. As a result, increasing unsaturation increases the likelihood of initiating oxidative damage in lipids. Propagation occurs when a lipid peroxyl combines with O_2 and forms a peroxyl radical ($ROO^{\bullet}$). This reaction becomes more likely when oxygen concentrations are high and can generate more ROS. Low oxygen concentration can favor the termination of lipid peroxidation when, instead of reacting with oxygen, a peroxyl radical reacts with another peroxyl radical and stabilizes. Termination can also occur when antioxidants, such as ascorbate, reduce $ROO^{\bullet}$ to ROOH.

Damage to proteins can occur chemically, by direct attack of radicals such as $OH^{\bullet}$, and to a lesser extent, non-radical ROS such as H_2O_2. Damage to proteins can also occur by secondary damage involving reaction with products of lipid peroxidation such as $ROO^{\bullet}$. ROS oxidize amino acid side chains within protein structures, creating covalent modifications and can attack peptide bonds, further compromising primary protein structure. Protein complexes, including complex I of the ETS, bind metal ions, especially iron and copper, that can generate localized $OH^{\bullet}$ when exposed to H_2O_2. Such damage can alter protein function by creating conformational changes that alter hydrophobic interactions, thereby reducing protein binding affinity and enzymatic activity, and causing protein aggregation. However, antioxidants (such as glutathione reductase) readily detoxify protein radicals to reduce propagation (26). Further, reactive electrons on protein side chains can migrate to and from other residues, mitigating further reactivity. Finally, protein carbonyls cannot diffuse across membranes like lipid peroxyls can (26),

containing protein carbonyl propagation. Therefore, while protein oxidation has many potential functional effects, it does not usually propagate to the extent of lipid peroxidation.

DNA is relatively stable and less susceptible to oxidative damage than lipids or protein. However, several ROS species can cause DNA damage that can be measured as strand breaks or chemical modification to DNA bases. For example, binding of metal ions to DNA makes it a target of ROS damage by site-specific $OH^{\bullet}$ generation, causing localized destruction in the form of base alterations, leading to base deletions and sometimes strand breaks. In particular, copper ions bind to GC-rich sequences in DNA thereby making these sequences a major target of $OH^{\bullet}$ damage. End products of lipid peroxidation can also modify DNA bases. Again, peroxyls are more likely to attack guanine, making it the most susceptible DNA base oxidation (44). However, the biological significance of oxidative damage depends on where the DNA damage occurs and how fast it is repaired.

1.12 Antioxidant Defense

Decreased oxidative damage, especially during arousal, may involve either a decrease in the proton motive force or an increase in antioxidant capacity. Increased antioxidant capacity could include increased production or activity of intracellular enzymatic antioxidants such as mitochondrial and cytosolic isoforms of superoxide dismutase, glutathione peroxidase, and catalase, as well as non-enzymatic antioxidants such as Vitamin E, and ascorbate (Vitamin C). See Figure 4.

Enzymatic antioxidants include mitochondrial manganese-dependent superoxide dismutase (MnSOD), which converts $O_2^{\bullet}$ to H_2O_2, and catalase that converts H_2O_2 to H_2O. Glutathione peroxidase is a cytosolic enzyme that catalyzes the reduction of hydrogen peroxide to water and oxygen. Some studies have shown increased concentrations of MnSOD and glutathione peroxidase during the hibernation season compared to summer (108), suggesting an increased production of antioxidants to mitigate ischemia-reperfusion like damages brought on by arousal to IBE (14). More recent work on TLGS does not support the hypothesis that hibernation is associated with

enhanced oxidative stress resistance due to an upregulation of intracellular antioxidant enzymes including SODs and glutathione peroxidase (83).

Non-enzymatic antioxidants in mitochondria include glutathione, vitamin C and vitamin E. The glutathione couple (GSSH/GSH) is an important non-enzymatic redox couple in the mitochondrial matrix that detoxifies ROS in combination with enzymatic antioxidants (glutathione reductase and glutathione peroxidase). Glutathione reductase reduces GSSG to GSH and also reduces the protein thioredoxin (that maintains reduced protein thiols). Using glutathione peroxidase, GSH detoxifies H_2O_2, that can be generated by SOD detoxification of superoxide (77; Figure 4). Vitamin E is localized to the IMM and limits the propagation of lipid peroxidation. Ascorbate is specific to the aqueous phase, or intermembrane space in isolated mitochondria and can both regenerate Vitamin E and scavenge free radicals directly. During arousal from torpor in arctic ground squirrels, when oxygen consumption is highest, and reperfusion damage is expected to be highest, ascorbate levels in blood progressively decrease to levels similar to summer ground squirrels, suggesting that plasma ascorbate accumulates before arousal and may protect metabolically active tissues from increased oxidative stress (31).

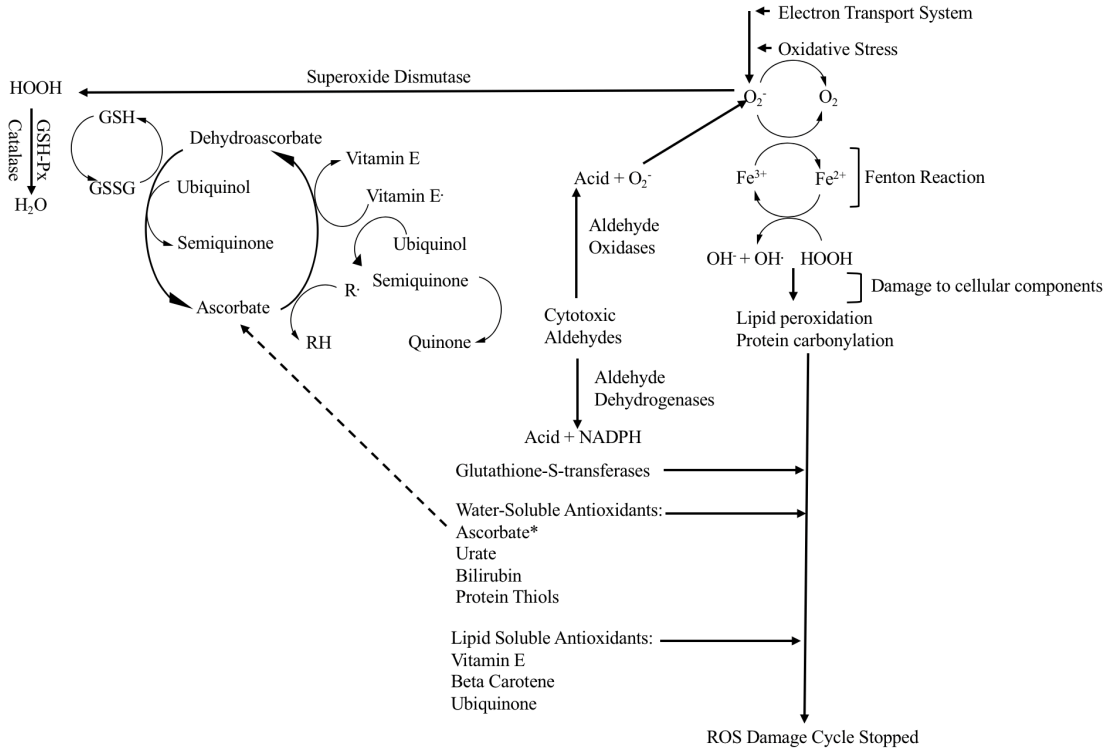

Figure 4. Systems for protection against reactive oxygen species. Superoxide is generated during metabolism from the electron transport system and increased with oxidative stress (such as anoxia-reoxygenation). Superoxide reduces Fe^{3+}, enabling it to enter into Fenton-type reactions, which produce hydroxyl radicals. This extremely reactive radical attacks cellular components (lipids, proteins, DNA), and initiates lipid peroxidative chain reactions. Cytotoxic aldehydes are end products of lipid peroxidation. When tissues are disrupted, aldehyde dehydrogenases are converted to aldehyde oxidases, which generate superoxide. Superoxide dismutase's (Mn or Cu) convert superoxide to peroxides (HOOH). Catalase and glutathione peroxidase convert peroxides to H_2O and O_2. Reduction of peroxides is accompanied by oxidation of reduced glutathione (GSH). GSH can be regenerated from glutathione disulfide (GSSG) by dehydroascorbate. Ascorbate (*) can react directly with free radicals and can regenerate vitamin E. Vitamin E can also directly react with free radicals. Glutathione S-transferases conjugate glutathione with peroxyl radicals. Aldehyde dehydrogenases convert aldehydes to less toxic products (ex. NADPH). Water and lipid soluble antioxidants listed can also react with free radicals to limit ROS damage. Modified from 71.

1.13 Objectives, hypotheses, predictions

Hibernators such as the TLGS have adapted to survive physiological challenges during cycles of torpor and interbout euthermia. Metabolic suppression allows TLGS to survive the low availability of food energy as well as hypoxia. However, the rapid changes in blood flow during arousals may still be detrimental because they can create mismatches between oxygen supply and demand and increased risk of oxidative damage. Such damage may be especially high in peripheral tissues that experience more drastic changes in blood flow, as well as in tissues that are highly active during arousals, such as brown adipose tissue, liver, and skeletal muscle. Although arousal is often considered analogous to ischemia-reperfusion (33; 7) the severity of oxidative damage to tissues and mitochondria during hibernation, and under anoxia followed by reoxygenation is not well documented.

In this study my primary goal was to compare the effects of the rapid and drastic changes in blood flow on oxidative damage among torpor, IBE, and summer TLGS. I also determined the functional impacts of anoxia-reoxygenation on isolated liver mitochondria from different hibernation states.

I hypothesize that:

1. A mismatch between oxygen supply and demand during hibernation will increase oxidative damage in tissue.
2. A) Anoxia-reoxygenation will increase ROS production in isolated mitochondria, leading to damage that will decrease maximal mitochondrial respiration.

   B) An exogenous antioxidant (ascorbate) will mitigate this ROS damage in all groups, dampening any decrease in maximal respiration.
3. Most ROS damage in anoxia-reoxygenation is generated by RET, which is mitigated by inhibiting complex I with rotenone.

I will explore these hypotheses via a series of objectives whereby I will compare torpid, IBE, and summer TLGS for the following:

1. Markers of ROS damage and antioxidant capacity in eight tissues,
2. Impacts of anoxia followed by reoxygenation on mitochondrial respiration and the potential for antioxidants to mitigate these effects,
3. Markers of ROS damage in mitochondria exposed to anoxia-reoxygenation.

I predict that:

1. Tissues from TLGS during the hibernating season, especially IBE, will have more oxidative damage than summer or non-hibernating animals, as summer squirrels do not experience the mismatch in oxygen supply produced during arousal, and therefore would likely generate fewer ROS. Lipid damage will be more prevalent than protein damage, because lipids are often more susceptible to ROS and DNA will be least damaged as it is least susceptible to ROS.
2. In isolated liver mitochondria subjected to anoxia-reoxygenation:
    A) maximum respiration rates (ST3), will be reduced following anoxia-reoxygenation, due primarily to oxidative damage to proteins, and membrane leak (ST4), will increase due to phospholipid damage. Due to the suppression of mitochondrial metabolism in torpor I predict these changes will be more drastic in IBE, and that winter phenotypes will be less affected than the summer phenotype.
    B) Addition of an exogenous antioxidant will mitigate reductions of ST3 following anoxia-reoxygenation and dampen increases of ST4 after anoxia-reoxygenation.
3. Mitochondria exposed to anoxia-reoxygenation will have increased levels of oxidative damage than freshly isolated mitochondria. There will be less oxidative damage to isolated mitochondria when complex I is inhibited by rotenone.

Chapter 2

2 Methods

2.1 Experimental animals

All experiments were performed in accordance with an approved Western University Animal Care Protocol (2012-016; see Appendix 1).

Ictidomys tridecemlineatus (thirteen-lined ground squirrels; TLGS) were born in captivity following established husbandry protocols (104), or were live-trapped in Carman, MB, Canada (49°30'N, 98°01'W) in May 2017 under the Manitoba Conservation collection permit number WB18908. TLGS were housed at Western University and monitored daily. All TLGS were individually housed in plastic shoebox-sized (26.7×48.3×20.3 cm high) cages with dried corn cob-bedding (Bed o' Cobs ¼", The Andersons, Maumee, OH), shredded paper nesting material (Crink-l' Nest, The Andersons, Inc.), and a length of PVC plastic tube (8 x 15 cm) as a refuge. Rat chow (LabDiet 5P000), dry dog food (Iams), and water were provided *ad libitum*. During the non-hibernating season (April-November 2018; April-November 2019; April 2020) TLGS were housed at 22 °C ± 3 °C with a photoperiod matching Carman, MB (adjusted weekly using full-spectrum fluorescent lighting). Transitioning to the hibernation season (November 2018; November 2019), animals were transferred to environmental chambers and the ambient temperature was lowered by 1 °C per day until 4 °C ± 2 °C was reached. During the hibernation season (November 2018-March 2019; November 2019-March 2020) TLGS were housed at 4 °C with a photoperiod set to 22 h dark:2 h light (with lights on at 12:00 h) to mimic TLGS burrow conditions and to allow for daily animal care monitoring. Lewis rats were donated by the Lawson research center.

2.2 Body temperature telemetry implants

Radiotelemeters (Models ETA-F10 or TA-F10, Data Sciences International, St. Paul, MN) were implanted in adult ground squirrels to measure core body temperature and monitor hibernation states. Squirrels were first induced with 4 % isoflurane gas anesthesia and maintained at 2 %. TLGS was then injected sub-cutaneously with slow

release buprenorphine (1 mg/kg) as an analgesic. The radiotelemeters were then implanted in the abdominal cavity through a 1 cm incision along the midline of the abdomen and abdominal wall. Abdominal wall and skin incisions were closed using absorbable suture (Johnson & Johnson 4-0 coated VICRYL Plus 27" VCP310). Sterile saline (5 ml) was administered subcutaneously to prevent dehydration and plastic cones were fitted around the neck to minimize biting of sutures for three days post-implantation. Core body temperature measurements were collected every ten minutes using telemetry receivers (model RA1010, Data Sciences International) using DataQuest ART software (Data Science International).

2.3 Experimental groups

This study compared TLGS in three experimental states: torpor (body temperature (t_b) = 5 °C for 3-5 days), inter-bout euthermia (IBE; t_b= 37 °C for 4-5 hours following arousal), and summer (n= 7, t_b= 37 °C for 4 months, April-July 2019). I also compared ground squirrels to non-hibernating rats (n= 5). Torpor TLGS samples were collected from January through March in 2019 (n= 7) and 2020 (n= 7). IBE samples were also collected from January through March in 2019 (n= 8) and 2020 (n= 9).

2.4 Tissue sampling

Torpid TLGS were euthanized by cervical dislocation because anesthetic injection would induce arousal. Squirrels sampled in IBE and summer were euthanized by intraperitoneal injections of Euthanyl (0.5 ml of 240 mg/ml; Bimeda-MTC, Cambridge ON) followed by cervical dislocation. The donated rats were kidney donors in separate experiments and received isoflurane anesthesia for kidney removal and then lethal Euthanyl injection. Liver was dissected immediately following euthanasia in ground squirrels and within 15 min following euthanasia in rats (see Appendix 3 RCRs). For both TLGS and rats a small section of the left liver lobe was frozen in liquid nitrogen for markers of oxidative damage assays. Seven additional tissues: forebrain, brainstem, brown adipose tissue, left ventricle, kidney, small intestine and gastrocnemius muscle were then immediately dissected and frozen in liquid nitrogen for oxidative damage assays.

2.5 Mitochondrial isolation

Immediately following excision from both TLGS and rats, liver was submerged in 20 ml of ice-cold homogenization buffer (HB; 250 mM sucrose, 10 mM HEPES, 1 mM EGTA, pH 7.4). Liver was then minced into 1 mm^3 pieces using surgical scissors and then transferred into a pre-chilled glass mortar and gently homogenized with three passes at 100 rpm with a pre-chilled Teflon pestle. The homogenate was then filtered through one layer of cheesecloth into two pre-chilled 50 ml polycarbonate centrifuge tubes and centrifuged at 4 °C and 1000 *g* for 10 min. The top fatty layer was aspirated from each tube, and the homogenate was then filtered through four layers of cheesecloth into two clean centrifuge tubes, and then centrifuged again at 4 °C and 1000 *g* for 10 min.

The supernatant was removed again, and the homogenate filtered through four layers of cheesecloth into clean tubes which were centrifuged at 8700 *g* for 10 min at 4 °C. The extra-mitochondrial supernatant was discarded, and the remaining mitochondrial pellet was re-suspended in 500 µl BSA-free HB. This crude mitochondrial sample was carefully layered into a centrifuge tube containing a Percoll (Sigma-Aldrich) solution gradient which consisted of four 10 ml layers of Percoll diluted with BSA-free HB to final Percoll concentrations of 10, 18, 30, 70 % (v/v). These tubes were then centrifuged at 35000 *g* for 35 min at 4 °C to obtain purified mitochondria, which settle between the 30 % and 70 % Percoll layers. The 70 % Percoll layer was then removed with a glass transfer pipette, and all layers above the settled mitochondria were aspirated.

The purified mitochondria sample was washed without resuspension with approximately 20 ml BSA-free HB and centrifuged twice more at 4 °C and 8700 *g* for 10 min to remove Percoll, and the extra-mitochondrial supernatant was replaced with fresh BSA-free HB between spins. The final mitochondrial pellet was re-suspended in 1 ml BSA-free HB and divided into 200 µl aliquots in pre-chilled 2.5 ml Eppendorf tubes. Mitochondria protein concentration was then determined using Bradford protein assay. Two aliquots were kept on ice for subsequent respirometry and the remainder were frozen at -80 °C for subsequent assays of oxidative damage markers.

2.6 Lipid Peroxyl Content

Oxidative damage to lipids was detected in homogenized tissue and isolated liver mitochondria using an assay kit (Abcam, ab118970) that measures levels of malondialdehyde (MDA), a marker for lipid peroxidation. In this assay thiobarbituric acid (TBA) reacts with MDA, forming MDA-TBA adducts which can be detected colorimetrically (553 nm). This method is also commonly known as a TBARS assay.

Approximately 0.1 g of forebrain, brainstem, brown adipose tissue, left ventricle, kidney, small intestine and gastrocnemius muscle tissues, frozen at -80 °C, were homogenized using a mini handheld homogenizer plastic pestle and Eppendorf tube in 303 µl of homogenization buffer (MDA lysis buffer from kit with 1% BHT (butylated hydroxytoluene, preventing MDA breakdown). The homogenate was then centrifuged at 13000 *g* for ten minutes at 4 °C. The supernatant was collected for the assay. Isolated liver mitochondria were thawed on ice after being held at -80 °C and vortexed before beginning the assay.

All reagents were equilibrated to room temperature prior to assay and each sample was analysed according to the protocol provided by the kit. A standard curve was produced for measuring total MDA with 0, 20 40, 60, 80 and 100 µM stock MDA supplied with the kit. 600 µl of TBA reagent (250 mg TBA dissolved in 7.5 ml glacial acetic acid) was added with 200 µl sample or standard, and in sample controls, 600 µl of glacial acetic acid was added in place of the TBA reagent into each 1.5 ml cryo tube and incubated at 95 °C for 60 min. Samples were then cooled to room temperature and centrifuged at 1000 *g* for 5 minutes at 4 °C to remove debris. Finally, 200 µl of supernatant were plated in duplicate into 96-well plates, and the absorbance was measured immediately at 532 nm using a SpectraMax plate spectrophotometer (Molecular Devices, Toronto ON) at 37 °C.

To remove background absorbance, mean sample control (sample homogenate without indicator, but with all other components) absorbance values were subtracted from mean sample values. Also, to remove background absorbance, in standard calculations, mean blank (0 µM MDA) standard values were subtracted from standard (20-100 µM

MDA) duplicates. Average corrected standard values were used to generate a standard curve and determine the amount of MDA (A). MDA concentration was then calculated by the following equation: MDA Concentration= (A / mg or ml) x 4 x dilution factor

2.7 Protein Carbonyl Content

Oxidative damage to proteins was detected in homogenized tissue and isolated liver mitochondria by measuring carbonyl groups, a marker of protein carbonylation using an assay kit (Cayman, 10005020). This assay uses the DNPH (2,4-dinitrophenylhydrazine) reaction with protein carbonyls, which forms a protein-hydrozone complex that can be measured using absorbance spectrophotometry at a wavelength of 375 nm. Duplicate measurements were standardized by tissue wet weight or mitochondrial protein concentration.

Approximately 200 mg of forebrain, brainstem, brown adipose tissue, left ventricle, kidney, small intestine and gastrocnemius muscle tissues, frozen at -80 °C were homogenized with a mini handheld homogenizer, plastic pestle and Eppendorf tube in 1 ml of ice cold phosphate buffer (PBS, pH 6.7, 1mM EDTA, 0.2M NaH_2PO_4, 0.2M $NaHPO_4$). Isolated liver mitochondria were thawed on ice after being held at -80 °C and vortexed before beginning the assay.

All reagents were equilibrated to room temperature prior to assay and each sample was analysed according to the protocol provided by the kit. A 100 µl aliquot of the homogenized tissue samples, 50 µl of isolated liver mitochondria, and 200 µl of diluted mitochondria (see section 2.9, below) were then transferred to two 1.5 ml microcentrifuge tubes (sample tube and control tube). Then, 400 µl of DNPH reagent (2,4-dinitrophenylhydrazine dissolved in 2.5M HCl) was added to the sample tubes, whereas 400 µl of 2.5 M HCl was added to the control tubes. Both sets of tubes were incubated in the dark at room temperature for 1 h, and vortexed every 15 min during the incubation. After incubation, 500 µl of 20 % trichloroacetic acid (TCA) was added to each tube, which were then vortexed and incubated on ice for 5 min. The tubes were then centrifuged at 10000 *g* for 10 min at 4 °C and the supernatant was discarded. The protein pellet was then resuspended in 500 µl of 10 % TCA and incubated on ice for 5 min. The

tubes were centrifuged again at 10000 *g* for 10 min at 4 °C, and the supernatant was discarded. The pellet was then re-suspended in 500 µl of ethanol/ethyl acetate (1:1) mixture and centrifuged at 10000 *g* for 10 min at 4 °C. This washing in ethanol/ethyl acetate was repeated twice more. After the final wash, protein pellets were resuspended in 500 µl of guanidine hydrochloride by vortex. Samples were centrifuged at 1000 *g* for 10 min at 4 °C to remove debris. Finally, 220 µl of supernatant was plated in duplicate in 96-well plates, and the absorbance was measured immediately at 375 nm using a SpectraMax plate spectrophotometer (Molecular Devices, Toronto ON) at 37 °C.

A corrected absorbance (CA) was calculated by subtracting control readings from sample absorbance readings. The concentration of carbonyls (nmol/ml) was determined by the following equation:

Protein Carbonyl (nmol/ml) = [(CA)/ (0.011 μM^{-1})] (TCA volume µl/ sample volume)

where 0.011 is a corrected extinction coefficient. These values were corrected for wet weight of homogenized tissue (nmol/g tissue) or for protein concentration of mitochondria (nmol/ mg protein).

2.8 DNA abasic sites

Oxidative damage to DNA was detected in DNA isolated from homogenized tissue, measuring apurinic/pyramidic (abasic; AP sites), a marker of DNA oxidation using an assay kit (Abcam, ab211154). This assay uses a probe that reacts specifically with an aldehyde group on the open ring form of AP sites and can be detected using absorbance spectroscopy at a wavelength of 450 nm.

DNA was isolated from tissue (approx. 0.1 g) by homogenization with DNAzol reagent (Genomic DNA isolation reagent, Fisher, 10503027). The DNA was precipitated from the homogenate with ethanol (70, 100 %). Following an ethanol wash, DNA was solubilized in 8 mM NaOH and adjusted to a final pH of 7.5. DNA results (purity and concentration) were quantified at an absorbance of 280 nm.

Purified DNA was diluted to 100 µg/ml in TE (Tris-EDTA) buffer. 5 µl of 100 µg/ml purified DNA was mixed with 5 µl of aldehyde reaction probe solution (provided with the kit) and incubated at 1 hour at 37 °C. 90 µl of TE buffer and 1 µl of glycogen solution (provided with the kit) were mixed, followed by 10 µl sodium acetate, then 300 µl of 100 % ethanol. This solution was then incubated at -20 °C for 30 minutes. The solution was then centrifuged for 15 minutes at 14000 *g* at 4 °C. The DNA was then washed three times in 70 % ethanol and spun at 1000 *g* to remove trace amounts of ethanol.

The DNA pellet was air dried and then dissolved in 30 µl TE buffer. DNA purity and concentration were then quantified again at an absorbance of 260/280 nm. DNA was then diluted to 1 µg/ml in TE buffer. 50 µl of samples (1 µg/ml DNA) or standards (0-20 µg/ml DNA), and 50 µl of DNA binding solution (supplied with the kit) was added to each well of a DNA high-binding plate for 2 h incubation at room temperature on an orbital shaker. Microwell strips (provided with the kit) were each washed in 250 µl of 1x wash buffer (provided with the kit), with aspirations between each wash. 100 µl of diluted streptavidin-enzyme conjugate (provided with the kit) was added to each well and incubated at 37 °C for 1 hour. Microwell strip washing was then repeated 3 times. Then 100 µl of substrate solution (provided with the kit) was added to dry wells and incubated for 20 minutes on an orbital shaker at room temperature. 100 µl of stop solution (provided with the kit) was then added to each well. Output was then measured immediately on immediately at 450 nm in a SpectraMax plate spectrophotometer (Molecular Devices, Toronto ON) at 23 °C.

Blank standard absorbance values were subtracted from each standard and sample reading. Standard readings were used to generate a standard curve. The corrected sample reading was applied to the standard curve to get the number of AP sites/10^5 bp.

2.9 Total antioxidant capacity

Total antioxidant capacity (including both small molecule and enzymatic antioxidants) were determined using a commercial kit (Abcam, ab65329). Antioxidants can reduce Cu^{2+} to Cu^{+}, which can be chelated by a colorimetric probe with a peak absorbance at 570 nm. The magnitude of this absorbance is proportional to the total antioxidant capacity.

The homogenates used for the protein carbonyl assay were also used for total antioxidant assay. A standard curve was produced for measuring total antioxidant capacity with 0, 12, 24, 36, 48, 60 µM Trolox, a potent non-enzymatic antioxidant. A 100 µl aliquot of either standard or homogenized sample was then plated in duplicate into 96-well plates. A working solution (100 µl of Cu^{2+}) was added to each well, mixed and incubated at room temperature for 90 min in the dark. The output was then immediately measured at 570 nm using a SpectraMax plate spectrophotometer (Molecular Devices, Toronto ON) at 37 °C.

Average standard values were used to generate a standard curve and determine total antioxidant capacity (TAC) in samples. TAC (in units of Trolox equivalent capacity) was calculated by the following equation:

TAC = (TAC in sample) / (Sample volume) x dilution factor

2.10 Respirometry

Mitochondrial oxygen consumption was measured using an Oxygraph-O2K high-resolution respirometer (Oroboros Instruments, Austria). The respirometer was calibrated with air-saturated buffer and oxygen depleted buffer (established using a yeast suspension). A volume of isolated mitochondria, usually approximately 30 µl, that yielded 0.4 mg protein was added to each chamber with 2 ml of respiration buffer (MiR05: 110 mM sucrose, 60 mM K-lactobionate, 20 mM HEPES, 20 mM taurine, 10 mM KH_2PO_4, 3 mM $MgCl_2$, 0.5 mM EGTA, 1 % (w/v) fatty-acid free BSA, pH 7.1) at a constant temperature of 37 °C, and with constant stirring at 750 rpm. All substrates were dissolved in respiration buffer and inhibitors were dissolved in ethanol. Respiration rates were determined using saturating concentrations of both complex I-linked (1 mM

pyruvate, 1mM malate) and complex II-linked (6 mM succinate). Respiration rates were also measured when only complex II was active by using a complex-I inhibitor (5 μM rotenone) and 6 mM succinate.

For measuring the effects of anoxia-reoxygenation on mitochondrial performance I modified a procedure initially used with mitochondria isolated from hypoxia-tolerant turtles (40) State 3 (maximal coupled respiration, ST3) rates were determined using saturating concentrations of ADP (0.1 mM) and state 4 (leak respiration, ST4) rates were established after the depletion of ADP by the mitochondria, resulting in a new steady-state respiration lower than ST3. Once ST4 was established the chambers were opened slightly and N_2 gas was injected into the gas space above the respiration buffer until the oxygen concentration decreased to less than 5 % of air saturation. The chambers were then closed, and mitochondrial respiration drove the oxygen concentration of each chamber to zero, resulting in anoxia. Anoxic conditions were maintained for five minutes. At this point, ascorbate (12 mM) was added as antioxidant treatment in some groups. The chambers were then opened and re-oxygenated to air saturation for five min. Then one chamber was closed and ST3 and ST4 respiration rates were then determined again by another addition of saturating ADP (0.1 mM). Mitochondria in the other chamber, along with respiration buffer, were removed after reoxygenation and snap frozen in liquid N_2. These “diluted mitochondria” were then stored at -80 °C for oxidative damage assays.

2.11 Statistical analysis

Statistical analysis was performed using R Studio (Version 1.3.1073). The ANCOVA and evaluation of estimated marginal means (EMM) model was used to describe the effects of the dependent variables, taking covariates and interactions into account, and estimated at values common to all groups. The F-statistic was used to determine how well the model fit the data set, and a p-value greater than 0.05 indicated that the covariates could not explain differential effects on anoxia. The F-statistic was used to determine how well the model fit the data set, and a p-value greater than 0.05 indicated that the covariates could not explain differential effects on anoxia. When ANCOVA models were not significant ($P>0.05$) further analysis of main effects included one-way ANOVAs, two-way ANOVAs, and paired t-tests. Tukey post-hoc tests determine between group and within group statistical differences. Data are expressed as individual values or mean ± SE.

Chapter 3

3 Results

3.1 Markers of oxidative damage in tissue

3.1.1 Lipid damage

Lipid peroxidation was not significantly affected by the covariates sex (ANCOVA; $F_{1,76}$= 0.77, P=0.385), time spent in hibernation ($F_{1,76}$= 1.104, P=0.297), and total body mass ($F_{1,76}$= 0.06, P=0.808). Overall, both tissue type (Two-way ANOVA: $F_{7,67}$= 4.89, P=0.0002) and hibernation state (Two-way ANOVA: $F_{2, 67}$=24.60, P<0.0001) had significant effects on lipid peroxidation levels. There was an interaction of tissue type and hibernation state ($F_{14,53}$=3.56, P<0.0001), therefore lipid data were then further analyzed within each tissue type using one-way ANOVAs and Tukey's Post-hoc tests (Figure 5A).

Hibernation state had significant effects in the following tissues: BAT ($F_{2,7}$=28.29, P=0.002), heart ($F_{2,7}$=12.63, P=0.005), liver ($F_{2,7}$=11.05, P=0.010), kidney ($F_{2,7}$=12.32, P=0.005). Whereas in forebrain ($F_{2,7}$= 3.75, P=0.078), brainstem ($F_{2,7}$=3.90, P= 0.082), and intestine ($F_{2,8}$=2.22, P=0.171) lipid damage was not significantly affected by hibernation state. Compared with torpor or summer, lipid peroxidation was significantly higher in IBE for the following tissues: BAT (by almost 4-fold), heart (more than 2-fold) and intestine (5-fold higher) (Tukey: P=0.004, P=0.002; P=0.003, P<0.0001; P=0.032, P=0.018). In kidney, lipid peroxidation was 10-fold higher in torpor (P=0.004) than summer (but not IBE), with a 10-fold increase. In gastrocnemius muscle, again lipid peroxidation was 5-fold higher in torpor than summer (P<0.0001) and also 3.5-fold higher in IBE (P=0.006) than summer. In summary, for most tissues oxidative damage to lipid was highest in IBE, while torpor had moderate damage, and summer had the least lipid damage.

3.1.2 Protein Damage

The following covariates: sex (ANCOVA, $F_{1,73}$=1.47, P=0.230), time since first torpor bout ($F_{1,73}$=0.02, P=0.878), and total body mass ($F_{1,73}$=0.36, P=0.550) had no significant effects on protein carbonyl levels. Overall, tissue type had a significant effect on lipid peroxidation levels (Two-way ANOVA: $F_{7,67}$= 4.89, P=0.0002) as did hibernation state (Two-way ANOVA: $F_{2, 67}$=24.60, P<0.0001). There was an interaction of tissue type and hibernation state ($F_{14,59}$=3.56, P<0.0001), therefore protein data were then further analyzed within each tissue type using one-way ANOVAs and Tukey's Post-hoc tests (Figure 5B).

Hibernation state had significant effects on the following tissues: brainstem ($F_{2,7}$=6.02, P= 0.030), heart ($F_{2,7}$=5.88, P=0.032), liver ($F_{2,9}$=5.40, P=0.030), and intestine ($F_{2,8}$=12.14, P=0.004). However, forebrain ($F_{2,11}$= 2.62, P=0.117), BAT ($F_{2,8}$=3.35, P=0.088), kidney ($F_{2,7}$=2.27, P=0.184), and gastrocnemius muscle ($F_{2,8}$=3.05, P=0.104) did not differ significantly by hibernation state. Summer protein carbonyl levels were approximately 2-fold less than IBE and torpor in forebrain, heart, liver, and gastrocnemius muscle (Tukey: P=0.033; P=0.016, P<0.0001; P=0.0003, respectively). Moreover, liver and gastrocnemius muscle carbonyl levels were significantly higher in torpor than IBE (P=0.031; P=0.022, respectively) by at least 2-fold. In general, oxidative protein damage across tissues was higher in the hibernation season than during summer.

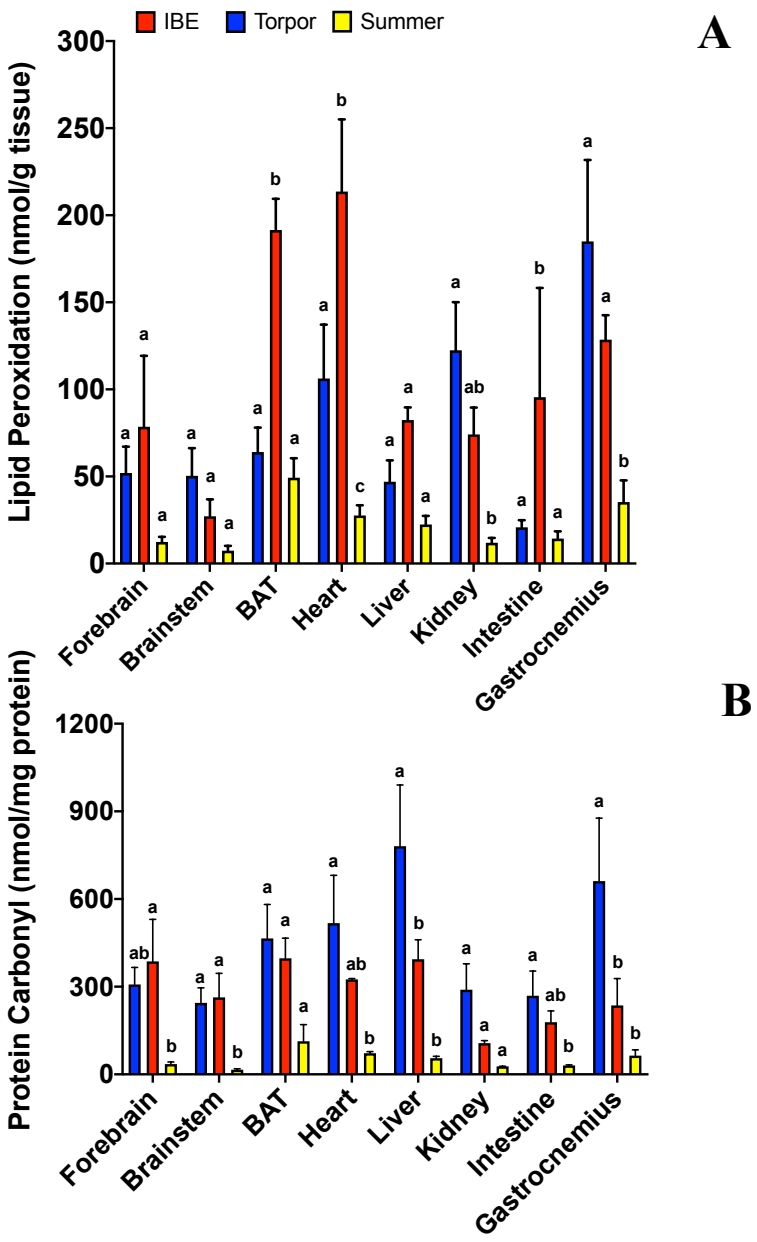

Figure 5. Markers of reactive oxygen species damage to lipids (A) and proteins (B) in 8 tissues of torpid, IBE and summer ground squirrels. Values are Mean ± SE. Lipid peroxyl (A), n=4 (all groups). Protein carbonyl (B), n=4. Groups that share the same letter are not significantly different within each tissue ($p \leq 0.05$; One-way ANOVAs and Tukey's Post-hoc test for each tissue type).

3.1.3 DNA damage

Neither sex, time in hibernation, nor total body mass had significant effects on the proportion of abasic (AP) sites in DNA (ANCOVA, $F_{1,35}= 1.13$, $P=0.297$; $F_{1,35}= 1.44$,

P=0.582; $F_{1,35}$= 3.10, P=0.582). Abasic sites were then analysed using a two-way ANOVA and Tukey's post-hoc tests, comparing both hibernation state and tissue type. There was no overall interaction of tissue type and hibernation state on AP sites (Figure 3, Two-way ANOVA: $F_{6,18}$=0.96, P=0.477). Overall hibernation state and tissue type had no overall effects on AP sites (Figure 6, Two-way ANOVA: $F_{2,6}$=2.05, P=0.210; $F_{3,18}$=0.59, P=0.588) and only one significant difference was found; in torpor, values in BAT were significantly lower than liver AP sites by 11 % (P=0.031).

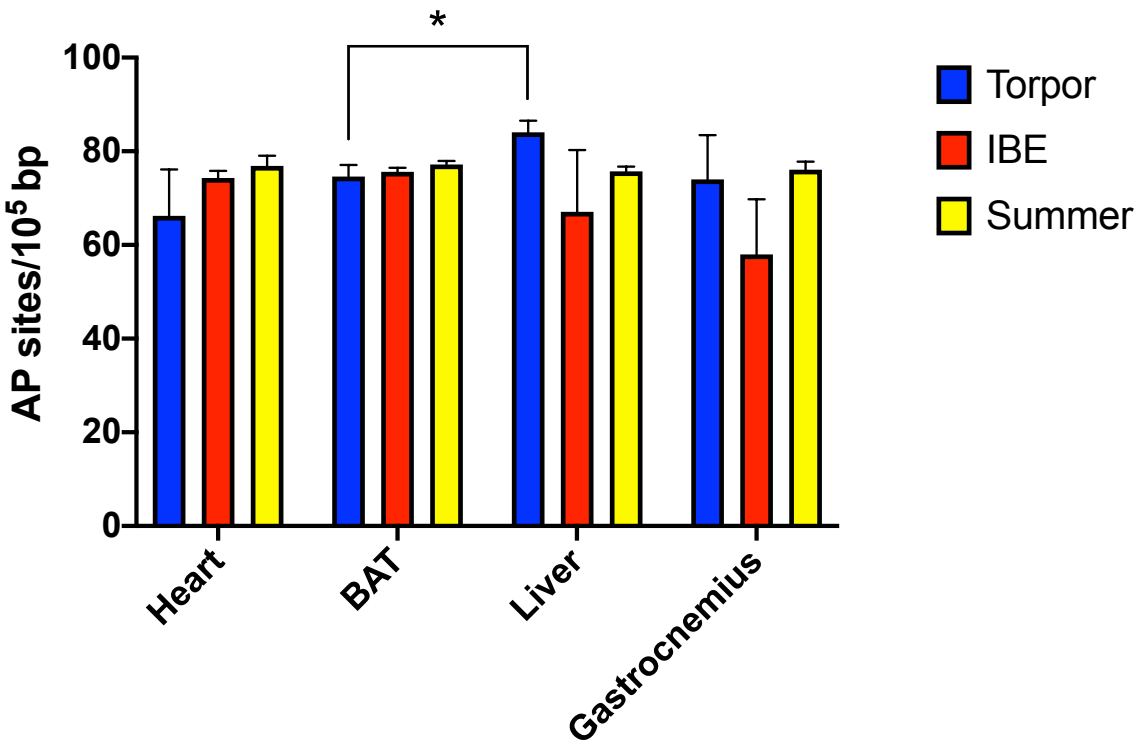

Figure 6. Apurinic/apyrimidinic (AP) sites of DNA damage in heart, brown adipose tissue, liver and gastrocnemius muscle of torpid, IBE and summer ground squirrels. Mean ± SE, n=3 (all groups). Asterisk represent significant difference ($p \leq 0.05$; Two-way ANOVA, Tukey's Post-hoc test).

3.1.4 Total antioxidant capacity

Neither sex, time in hibernation, nor total body mass had significant effects on total antioxidant capacity (TAC) (ANCOVA, $F_{2,89}$= 0.68, P=0.412; $F_{2,89}$= 0.22, P=0.637; $F_{2,89}$= 0.001, P=0.979). Two-way ANOVA showed no overall effect of hibernation state

($F_{2,83}$= 2.86, P=0.063), or interaction ($F_{14,66}$=1.73, P=0.07), but tissue type did have a significant effect ($F_{7,83}$= 5.79, P<0.0001).

Within each tissue, data was analysed using a one-way ANOVA and Tukeys-Post-hoc tests. Hibernation state had an overall effect on TAC of tissues (Figure 7, One-way ANOVA: $F_{2,66}$=5.30, P=0.007). Summer kidney TAC levels were 1.5-fold higher than torpor and IBE (Tukey: P=0.002; P=0.001). No other comparisons within tissue type showed any significant differences. Therefore, across all states, antioxidant response did not appear to vary.

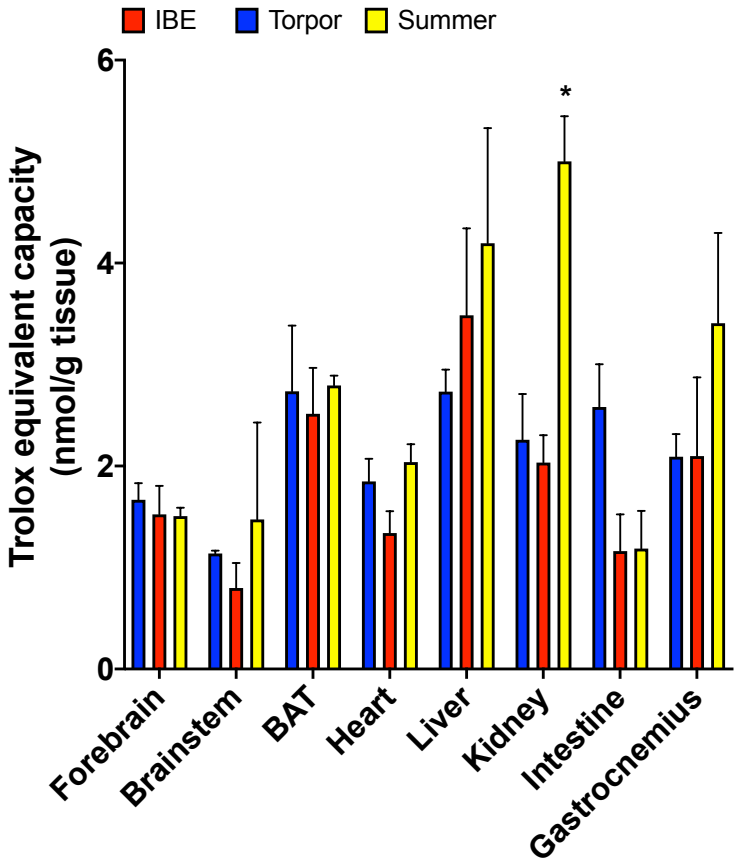

Figure 7. Total antioxidant capacity (Trolox equivalent capacity) in 8 tissues of torpid, IBE and summer ground squirrels, Mean ± SE. N=4 (all groups). Asterisk represents significant difference between hibernation groups in that tissue (p≤0.05; One-way ANOVA, Tukey's Post-hoc test for each tissue).

3.2 Mitochondrial Respiration

3.2.1 Effect of anoxia reoxygenation on respiration

Initially, I compared respiration rates of freshly isolated liver mitochondria without exposure to anoxia-reoxygenation. With both complex I-linked (pyruvate) and complex II-linked (succinate) substrates, maximal ADP-stimulated respiration rates (State 3; ST3) differed significantly among groups (Figure 8A; One-way ANOVA: $F_{3,40}$=14.22, P<0.0001). Initial ST3 in torpor was approximately 50 % lower than IBE (Tukey: P<0.0001) and summer (P<0.0001). IBE and summer ST3 did not differ significantly (P=0.994). Initial ST3 in rat was not significantly different from any initial TLGS rate (Torpor, P=0.441; IBE, P=0.083; Summer P=0.084).

With complex I-inhibited (by addition of rotenone) and a complex II-linked substrate (succinate), there was a similar pattern in initial respiration rates. Initial ST3 rates differed among groups (Figure 8B; One-way ANOVA: $F_{3,33}$=6.64, P=0.001), again being approximately 50 % lower in torpor than IBE (P=0.002) and summer (P=0.025) and there was again no significant difference between IBE and summer ST3 (P=0.989). Initial ST3 in rat was significantly higher than torpor by 51 % (P=0.024), but not significantly different than IBE (P=0.991) or summer (P=0.958).

With pyruvate and succinate as substrates, mitochondrial leak respiration (State 4; ST4) was significantly different among groups (Figure 9A; One-way ANOVA: $F_{3,39}$=4.69, P=0.007). In addition, rotenone inhibition of complex I combined with provision of succinate as substrate revealed that ST4 was significantly different among hibernation states (Figure 9B; One-way ANOVA: $F_{3,33}$=3.82, P=0.019). Initial ST4 values using pyruvate and succinate as a substrate were 37 % greater in IBE compared to torpor (P=0.023), and 60 % greater compared to rat (P=0.024), but there was no significant difference between IBE and summer ST4 (P=0.829). With rotenone addition and succinate as substrate, initial ST4 in IBE was 38 % greater than torpor (P=0.037) but there was no significant difference between IBE and summer ST4 (P=0.829). Initial ST4 with rotenone and succinate in rat was not significantly different than any initial ST4 in TLGS including IBE (0.087), torpor (P=0.090) or summer (P=0.154) states.

After establishing respiration rates of freshly isolated mitochondria, I tested how anoxia followed by reoxygenation would affect these rates. I hypothesized that metabolic suppression in torpor would mitigate damage upon reoxygenation. However, with the differences among initial respiration rates between individuals, post-anoxia reoxygenation rates likely depend on pre-anoxia values, potentially masking any effects of anoxia-reoxygenation. To account for this possibility, I analysed these data using a Two-way ANCOVA model with initial rates as covariates. With both pyruvate and succinate as substrates there was a significant effect of initial ST3 rates on post-anoxia rates ($F_{1,36}$=62.32, P<0.0001), but hibernation state did not have a significant effect ($F_{3,36}$=1.62, P=0.202). The interaction of hibernation state and initial ST3 approached significance ($F_{3,36}$=2.51, P=0.074) for ST3 fueled by both pyruvate and succinate. One-way ANCOVA analysis with the initial rate covariate (interaction removed), showed that hibernation state had a significant effect on post anoxia-reoxygenation rates ($F_{3,39}$=8.99, P=0.0001).

With succinate as substrate (in the presence of rotenone), Two-way ANCOVA with initial rates as covariates again show a significant effect of initial ST3 rates ($F_{1,29}$=51.64, P<0.0001) but not hibernation state ($F_{3,29}$=0.31, P=0.802) on post-anoxia ST3 rates. The interaction of hibernation state and initial ST3 state was not significant ($F_{3,29}$=2.02, P=0.133) and removed from further analysis. One-way ANCOVA showed that hibernation state had a significant effect on post anoxia-reoxygenation ST3 rates ($F_{3,32}$=12.27, P<0.0001).

Because ANCOVA showed that initial ST3 rates significantly affected post-anoxia rates, I calculated estimated marginal means to compare groups at initial ST3 values common to all groups (Table 1). With pyruvate and succinate as substrates ST3 respiration in rat mitochondria was significantly lower following anoxia-reoxygenation than any TLGS group. ST3 estimated marginal mean values were 43 % lower following anoxia-reoxygenation in rat than IBE (P=0.001), 50 % lower than torpor (P<0.0001), and 41 % lower than summer (P=0.005). However, within TLGS, estimated marginal mean values did not differ significantly among hibernation conditions (Table 1).

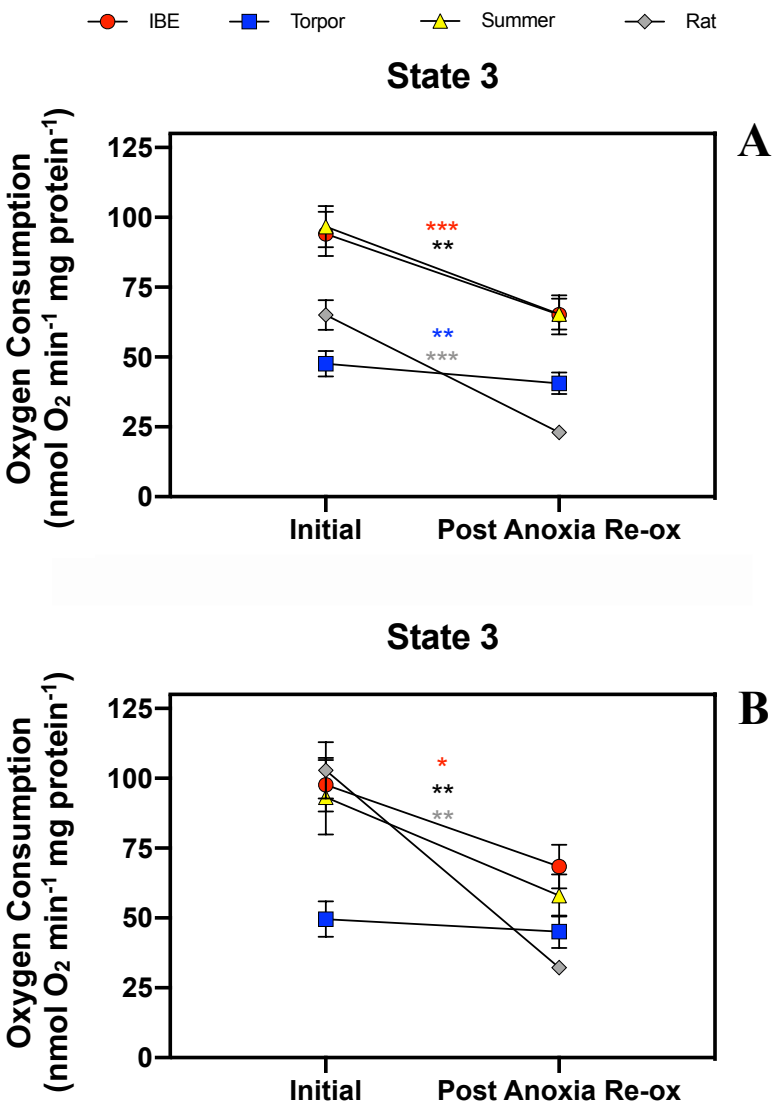

Figure 8. The effect of anoxia-reoxygenation on maximal respiration (state 3) rates in isolated liver mitochondria of IBE, torpor, summer TLGS and rat. Mitochondria were provided with pyruvate and succinate (A) or succinate in the presence of rotenone (B). Mean ± SE, n_{torpor}=17, n_{IBE}=14, n_{summer}=8, n_{rat}=5. Asterisks (red=IBE, blue=torpor, black=summer, grey=rat) indicates a significant decrease between initial (before anoxia) and post anoxia-reoxygenation ($p \leq 0.05$; *$p<0.05$, ** $p<0.001$, *** $p<0.0001$, paired, one-sided t-test).

Table 1. Estimated marginal means (EMM) of post anoxia reoxygenation ST3 respiration.

$N_{TorporPMS}$=7, $N_{TorporRS}$=3, N_{IBE}=7, N_s=7, N_R=5. Estimated marginal means (EMM) describe the effect of the dependent variable (post anoxia rates) taking the covariate (pre anoxia rates) into account. Groups that share the same letter are not significantly different (ANCOVA, P<0.05) when both pyruvate and succinate, or succinate alone (in the presence of rotenone) fueled respiration.

Hibernation State	Pyruvate and Succinate EMM (nmol O_2 min^{-1} mg $protein^{-1}$)	Rotenone and Succinate EMM (nmol O_2 min^{-1} mg $protein^{-1}$)
IBE	50.688 ± 3.34^{a}	69.164 ± 3.95^{ab}
Torpor	58.482 ± 3.31^{a}	69.963 ± 6.37^{a}
Summer	49.051 ± 4.28^{a}	49.796 ± 4.02^{b}
Rat	28.80 ± 4.96^{b}	17.06 ± 5.39^{c}

Post anoxia-reoxygenation pyruvate and succinate associated state 4 rates were significantly affected by initial ST4 rates (Two-way ANCOVA, $F_{1,35}$=752.79, P<0.0001), but hibernation state ($F_{3,35}$=1.511, P=0.229) and the interaction ($F_{3,35}$=0.23, P=0.233) were not significant. With the interaction of hibernation state and initial ST4 rate removed from the model, hibernation state had a significant effect (One-way ANCOVA, $F_{3,38}$=13.63, P<0.0001). Succinate (with rotenone) fueled ST4 rates showed the same relationship (Two-way ANCOVA, $F_{1,29}$= 361.45, P<0.0001; $F_{3,29}$=0.14, P=0.934; $F_{3,29}$=0.48, P=0.701; One-way ANCOVA, $F_{3,32}$=5.51, P=0.004) respectively.

At an initial ST4 value common to all groups (Table 2) estimated marginal means of IBE with pyruvate and succinate as substrates, were 13.5 % lower than torpor (P<0.0001), and 13 % lower than summer (P<0.0001). Initial torpor ST4 was not significantly different than summer (P=0.421), but rat was significantly lower than torpor by 13 % and summer by 13 % (P=0.002; P=0.028), and not significantly different than IBE (P=0.529). When complex I was inhibited, torpor ST4 was significantly higher than all groups (Figure 9A; IBE by 13 %, P=0.008; Summer by 12 %, P=0.023; Rat by 23 %, P=0.001).

To further analyse the effects of anoxia-reoxygenation on mitochondrial respiration I compared changes of mean rates within each hibernation state. With complex-I and -II substrates (pyruvate and succinate) ST3 rates decreased significantly following anoxia-reoxygenation in all groups (Figure 8A). Anoxia reduced ST3 by 16 % in torpor, and 33 % in both IBE and summer (Paired, one-sided t-test; P<0.0001). Rat ST3 was reduced by 65 % (P=0.002; P=0.0003). A similar pattern emerged with complex-I inhibited (rotenone) and succinate as substrate. ST3 decreased significantly after anoxia in all groups (Figure 8B), but torpor showed the smallest relative change 9 % (Paired, one-sided t-test; P=0.0008) compared with 30 % in IBE (P<0.0001), 38 % in summer (P=0.003) and 69 % in rat (P=0.002).

With pyruvate and succinate as substrates, leak respiration rates (ST4; Figure 9A) following anoxia reoxygenation were significantly higher in torpor (21 %) and summer (17 %) (Figure 9A; Paired, one-sided t-test; $P<0.0001$; $P=0.001$) but not in IBE or in rats ($P=0.072$; $P=0.195$). With rotenone and succinate (Figure 9B), ST4 increased in all TLGS groups post anoxia-reoxygenation IBE (5.4 %; $P=0.002$), Torpor, (21 %, $P<0.0001$), and summer (17 %, $P=0.019$), but rats again did not show an increase in ST4, despite approaching statistical significance ($P=0.052$).

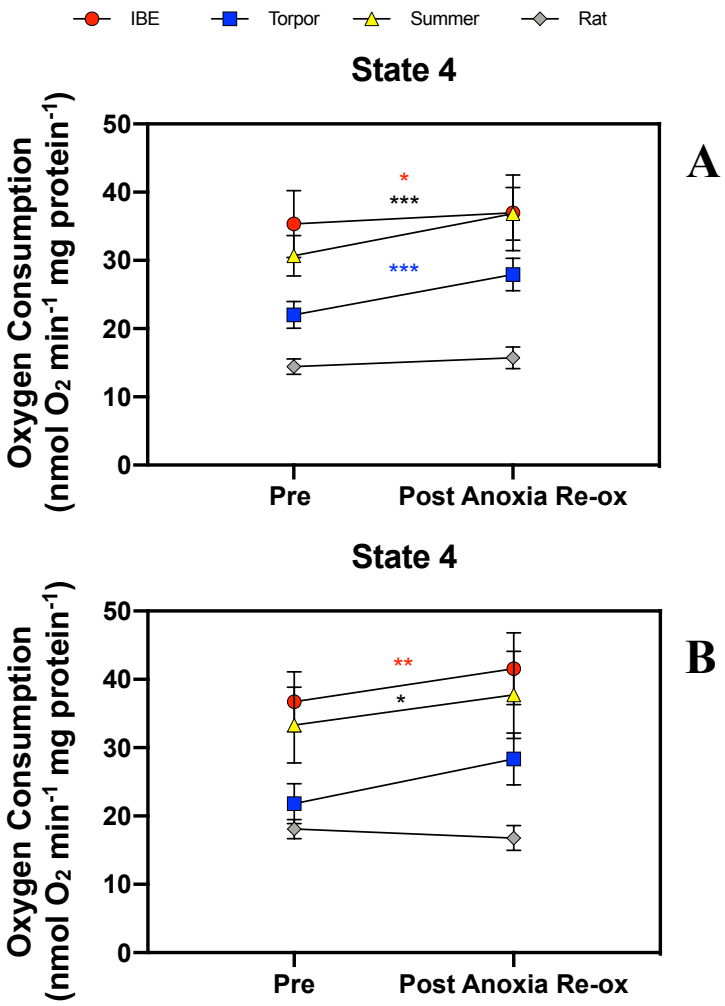

Figure 9. The effect of anoxia-reoxygenation on leak respiration (state 4) rates in isolated liver mitochondria of IBE, torpor, summer TLGS and rat. Mitochondria were provided with pyruvate and succinate (A) or succinate in the presence of rotenone (B). Mean ± SE, n_{torpor}=17, n_{IBE}=14, n_{summer}=8, n_{rat}=5. Asterisks (red=IBE, blue=torpor, black=summer) indicates a significant increase from initial (before anoxia) and post anoxia-reoxygenation ($p \leq 0.05$; *$p<0.05$, ** $p<0.001$, *** $p<0.0001$, paired, one-sided t-test).

Table 2. Estimated marginal means (EMM) of post anoxia reoxygenation ST4 respiration.
$N_{TorporPMS}$=7, $N_{TorporRS}$=3, N_{IBE}=7, N_s=7, N_R=5. Estimated marginal means (EMM) describe the effect of the dependent variable (post anoxia rates) taking the covariate (pre anoxia rates) into account. Groups that share the same letter are not significantly different (ANCOVA, P<0.05) when both pyruvate and succinate, or succinate alone (in the presence of rotenone) fueled respiration.

Hibernation State	Pyruvate and Succinate EMM (nmol O_2 min^{-1} mg $protein^{-1}$)	Rotenone and Succinate EMM (nmol O_2 min^{-1} mg $protein^{-1}$)
IBE	28.91 ± 1.14^a	32.71 ± 1.45^a
Torpor	33.44 ± 1.06^b	37.53 ± 2.12^b
Summer	33.21 ± 0.99^b	32.92 ± 1.39^a
Rat	29.09 ± 1.47^a	29.91 ± 1.90^a

3.2.2 Effect of the antioxidant Ascorbate on anoxia-reoxygenated mitochondria

Reduced ascorbate undergoes some uncatalyzed chemical oxidation in aqueous solution, so I corrected all respiration values in the presence of ascorbate for this effect by subtracting O_2 consumption rates after ascorbate was added to the chamber containing only MiR05 buffer. Further, like the previous section, post anoxia-reoxygenation rates are affected by initial rates before anoxia, ascorbate addition, and reoxygenation, so for comparison of post-anoxia reoxygenation rates I used a Two-way ANCOVA analysis with initial rates as covariates and initial rate interaction with hibernation state.

With both pyruvate and succinate as substrates there was a significant effect of initial ST3 rates ($F_{1,10}$=32.21, P=0.0002) but hibernation state did not have a significant effect ($F_{1,10}$=2.55, P=0.141). The interaction of hibernation state and initial ST3 rate was not significant ($F_{1,10}$=2.51, P=0.074) and was removed from the model. One-way ANCOVA analysis with the initial rate covariate, showed that hibernation state had a significant effect on post anoxia-reoxygenation rates ($F_{3,39}$=8.99, P=0.0001).

Using this ANCOVA model, I compared post anoxia-reoxygenation IBE and Torpor ST3 values at a common initial value of 78.5 nmol O_2 min^{-1} mg $protein^{-1}$, and determined that there was no significant difference in these estimated marginal means among hibernation states with pyruvate and succinate as substrates (Table 3, P=0.218). With rotenone inhibition combined with the succinate substrate were compared with a common initial value of 85.0 nmol O_2 min^{-1} mg $protein^{-1}$, IBE was 30 % lower than torpor, with ascorbate, IBE was 15 % lower than torpor (Table 3, P<0.0001). (Table 3, P=0.481).

In both IBE and torpor, ascorbate addition mitigated the decline in ST3 post-anoxia (Figure 10A) both during torpor and IBE. With both pyruvate and succinate ascorbate additions decreased the significant effect of anoxia-reoxygenation on ST3 respiration from 38 % (Paired, one-sided t-test: P<0.0001) to 30 % (P=0.002). In torpor, anoxia-reoxygenation significantly decreased ST3 by 13 % (P_T =0.001), but this treatment had no significant effect (P=0.475) when ascorbate was added.

Ascorbate protected ST3 more when complex-I was inhibited with rotenone than when complex I was active. In mitochondria isolated from IBE animals, and with succinate (in the presence of rotenone) as substrate, anoxia-reoxygenation significantly decreased ST3 by 41 % (Figure 10B; Paired, one-sided t-test: $P<0.0001$). The addition of ascorbate during anoxia lessened this decrease to 25 %, but it was still statistically significant ($P=0.005$). In torpor, anoxia-reoxygenation significantly decreased ST3 by 9 % ($P=0.003$), but the addition of ascorbate after anoxia eliminated this difference ($P=0.983$).

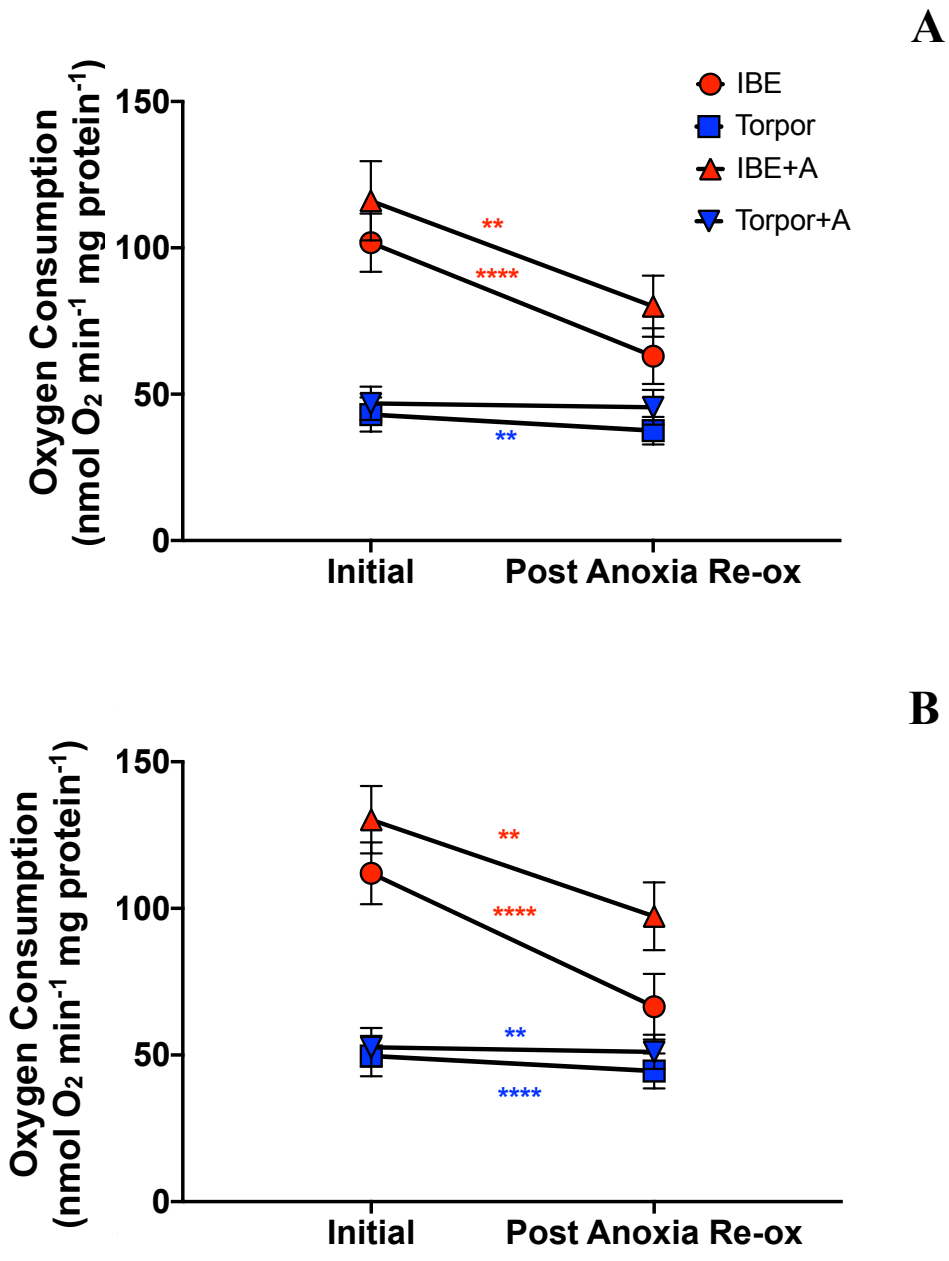

Figure 10. Effect of ascorbate maximal respiration (State 3) rates after anoxia-reoxygenation in isolated liver mitochondria of IBE and torpor ground squirrels. Mitochondria were provided with pyruvate and succinate (A) or rotenone and succinate (B). Mean ± SE, n_{torpor}=9, n_{IBE}=7. +A represents addition of ascorbate before reoxygenation. Asterisk indicates a significant increase between initial and post anoxia-reoxygenation without ascorbate ($p \leq 0.05$; *$p<0.05$, ** $p<0.01$, ***$p<0.001$, ****$p<0.0001$, paired, one-sided t-test).

Table 3. Estimated marginal means (EMM) of post anoxia reoxygenation ST3 respiration. Estimated marginal means (EMM) describe the effect of the dependent variable (post anoxia rates) taking the covariate (pre anoxia rates) into account. Groups that share the same letter are not significantly different (ANCOVA, $P<0.05$) when both pyruvate and succinate, or succinate alone (in the presence of rotenone) fueled respiration with the addition of antioxidant ascorbate (+Ascorbate) $n_{torpor}=9$, $n_{IBE}=7$.

Hibernation State	Pyruvate and Succinate EMM (nmol O_2 min^{-1} mg $protein^{-1}$)	Rotenone and Succinate EMM (nmol O_2 min^{-1} mg $protein^{-1}$)
IBE	46.761 ± 5.25^{a}	48.091 ± 4.59^{a}
Torpor	58.482 ± 3.31^{a}	68.594 ± 4.59^{b}
IBE +Ascorbate	54.171 ± 6.57^{a}	66.506 ± 9.41^{a}
Torpor +Ascorbate	68.219 ± 5.97^{a}	78.044 ± 8.47^{b}

Initial ST4 also had a significant effect on post anoxia-reoxygenation when ascorbate was added. ST4 with both pyruvate and succinate (Figure 11A; One-way ANCOVA: $F_{2,12}$=83.14 P<0.0001), and with only succinate (Figure 11B; One-way ANCOVA: $F_{2,12}$=18.03 P=0.001).

Using this ANCOVA model, I compared post anoxia-reoxygenation IBE and Torpor ST4, and determined that IBE was 22 % lower than torpor (P=0.04), but all other estimated marginal means were not different among hibernation states with pyruvate and succinate as substrates (Table 4). There was no significant difference among hibernation states when rotenone inhibition combined with the succinate substrate were compared (Table 4).

With pyruvate and succinate, IBE ST4 did not significantly change following anoxia-reoxygenation (Figure 11A) without (P=0.424) or with (P=0.069) ascorbate. In torpor, ST4 increased significantly in the absence of ascorbate (Figure 11A, P<0.0001) but ascorbate eliminated this effect (P=0.136).

With rotenone inhibition of complex-I and succinate as substrate, IBE ST4 (Figure 11B) did not increase without or with ascorbate (P=0.063; P=0.339). However, torpor ST4 increased significantly in the absence of ascorbate (P<0.0001) and increased with ascorbate, although to a lesser extent (P=0.015).

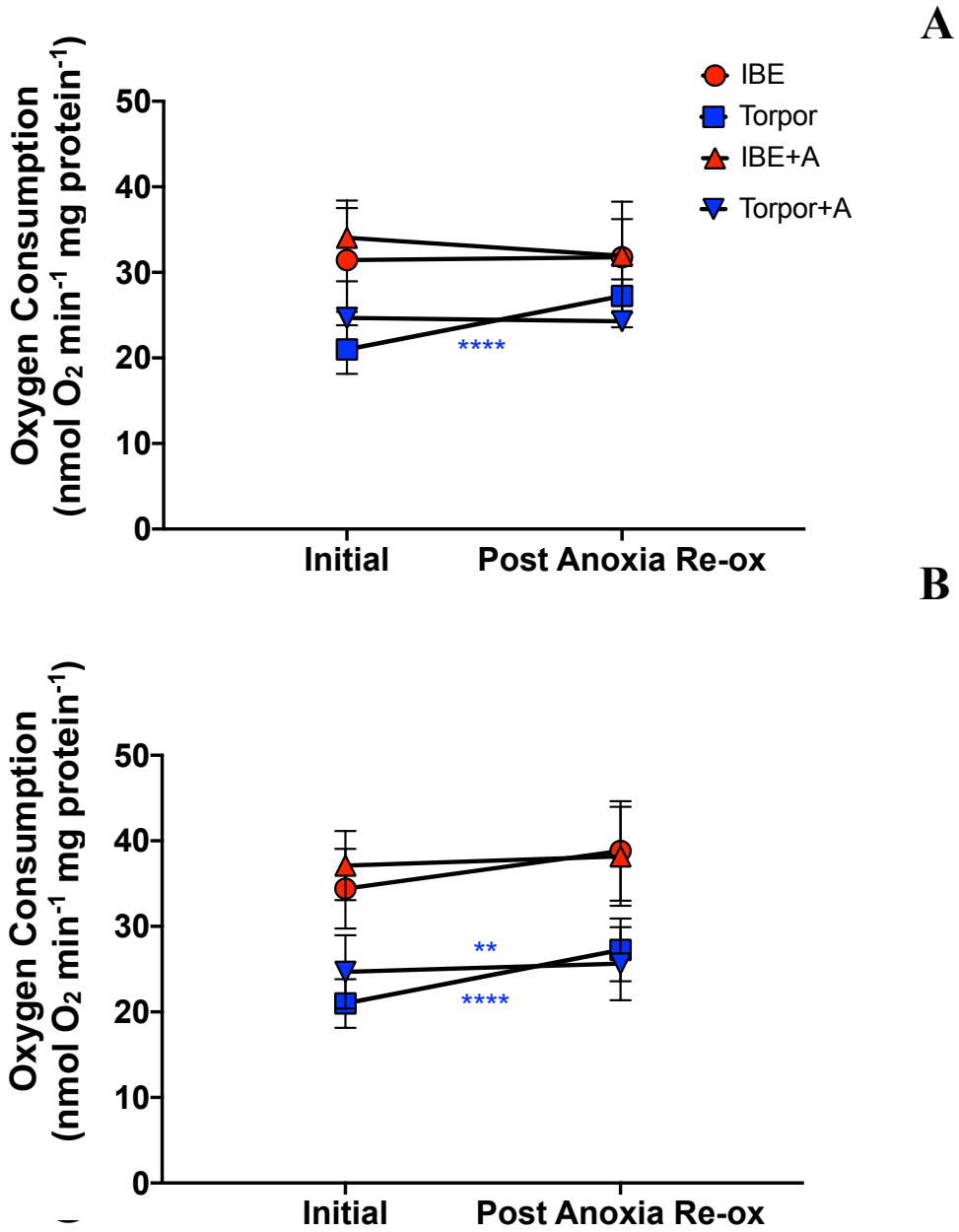

Figure 11. Effect of ascorbate on leak respiration (state 4) rates after anoxia-reoxygenation in isolated liver mitochondria of IBE and torpor ground squirrels. Mitochondria were provided with pyruvate and succinate (A) or rotenone and succinate (B). Mean ± SE, n_{torpor}=9, n_{IBE}=7. +A represents addition of ascorbate before reoxygenation. Asterisk indicates a significant increase between initial and post anoxia-reoxygenation without ascorbate ($p \leq 0.05$; *$p<0.05$, ** $p<0.01$, ***$p<0.001$, ****$p<0.0001$, paired, one-sided t-test).

Table 4. Estimated marginal means (EMM) of post anoxia reoxygenation ST4 respiration. Estimated marginal means (EMM) describe the effect of the dependent variable (post anoxia rates) taking the

Hibernation State	Pyruvate and Succinate EMM (nmol O_2 min^{-1} mg $protein^{-1}$)	Rotenone and Succinate EMM (nmol O_2 min^{-1} mg $protein^{-1}$)
IBE	24.98 ± 1.25^{a}	30.48 ± 1.63^{a}
Torpor	32.27 ± 1.09^{b}	34.50 ± 1.44^{a}
IBE +Ascorbate	25.03 ± 1.93^{a}	28.53 ± 2.18^{a}
Torpor +Ascorbate	30.36 ± 1.79^{ab}	34.03 ± 2.01^{a}

covariate (pre anoxia rates) into account. Groups that share the same letter are not significantly different (ANCOVA, $P<0.05$) when both pyruvate and succinate, or succinate alone (in the presence of rotenone) fueled respiration with the addition of antioxidant ascorbate (+Ascorbate) $n_{torpor}=9$, $n_{IBE}=7$.

3.3 Markers of oxidative damage in isolated mitochondria

3.3.1 Freshly isolated mitochondria

Lipid peroxidation levels in freshly isolated liver mitochondria did not differ significantly among hibernation states (Figure 12A; One-way ANOVA, $F_{2,5}$=3.52, P=0.111). Protein carbonyl levels were also not significantly different (Figure 12B; One-way ANOVA, $F_{3,15}$=0.10, P=0.957).

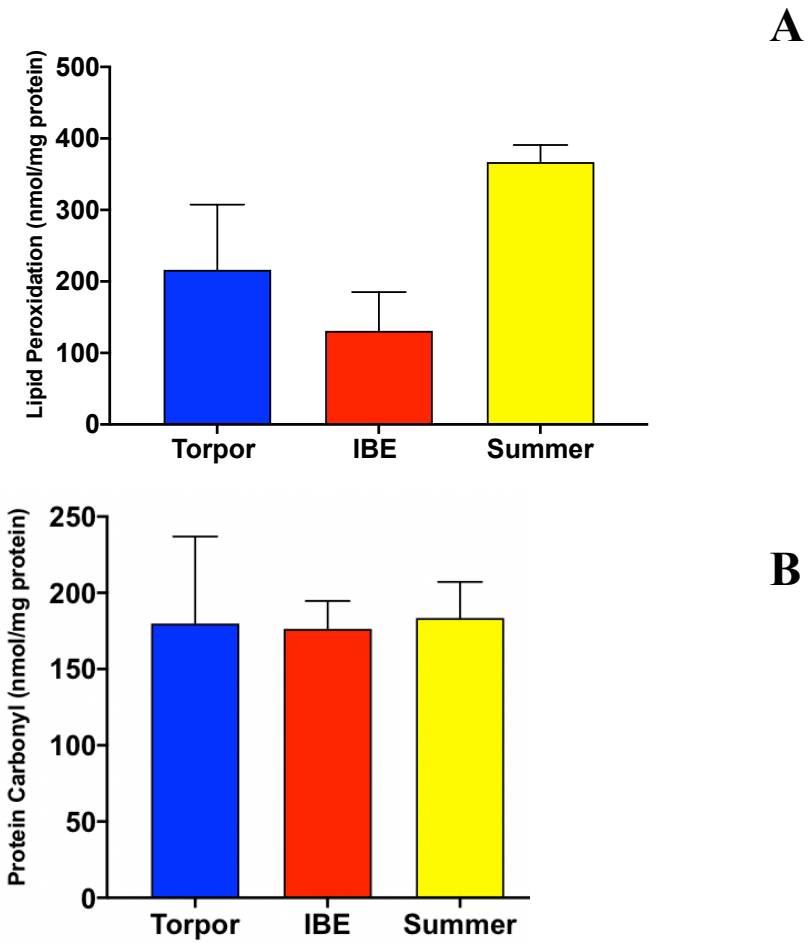

Figure 12. Markers of reactive oxygen species damage to proteins (A) and lipids (B) in freshly isolated liver mitochondria from torpor, IBE and summer ground squirrels. Mean ± SE, n=4 (all groups).

3.3.2 Damage to mitochondria following anoxia-reoxygenation

Protein carbonyl levels of anoxia-reoxygenated mitochondria were also analysed using a repeated measures two-way ANOVA and Tukey post-hoc tests (Figure 13A). There was also no interaction between hibernation state and substrate on protein damage ($F_{2,7}$=0.31, P=0.742). Hibernation state did not affect the results ($F_{2,7}$=0.17, P=0.848), but again, oxidative substrate (pyruvate and succinate vs. succinate in the presence of rotenone) did have an overall effect on damage ($F_{1,7}$=6.80, P=0.035). However, there were no significant differences in protein damage between the substrate treatments within each hibernation group.

Lipid peroxidation levels after 5 min anoxia followed by reoxygenation were analysed using a repeated measures two-way ANOVA and Tukey post-hoc tests (Figure 13B). There was no interaction between hibernation state and oxidative substrates on mitochondrial lipid damage ($F_{2,9}$=2.36, P=0.150). Hibernation state did not have a significant effect on lipid peroxidation levels ($F_{2,9}$=3.11, P=0.094). However, substrate did have a significant effect on lipid peroxidation levels ($F_{1,9}$=9.63, P=0.013). In summer, reoxygenation following anoxia increased lipid peroxidation levels 1.5-fold with pyruvate and succinate as substrates compared to summer with rotenone inhibition and succinate as substrate (P=0.020). Also, with rotenone inhibition and succinate substrate, mitochondrial lipid peroxidation levels in summer were significantly less than IBE (by 64 %) (P=0.013).

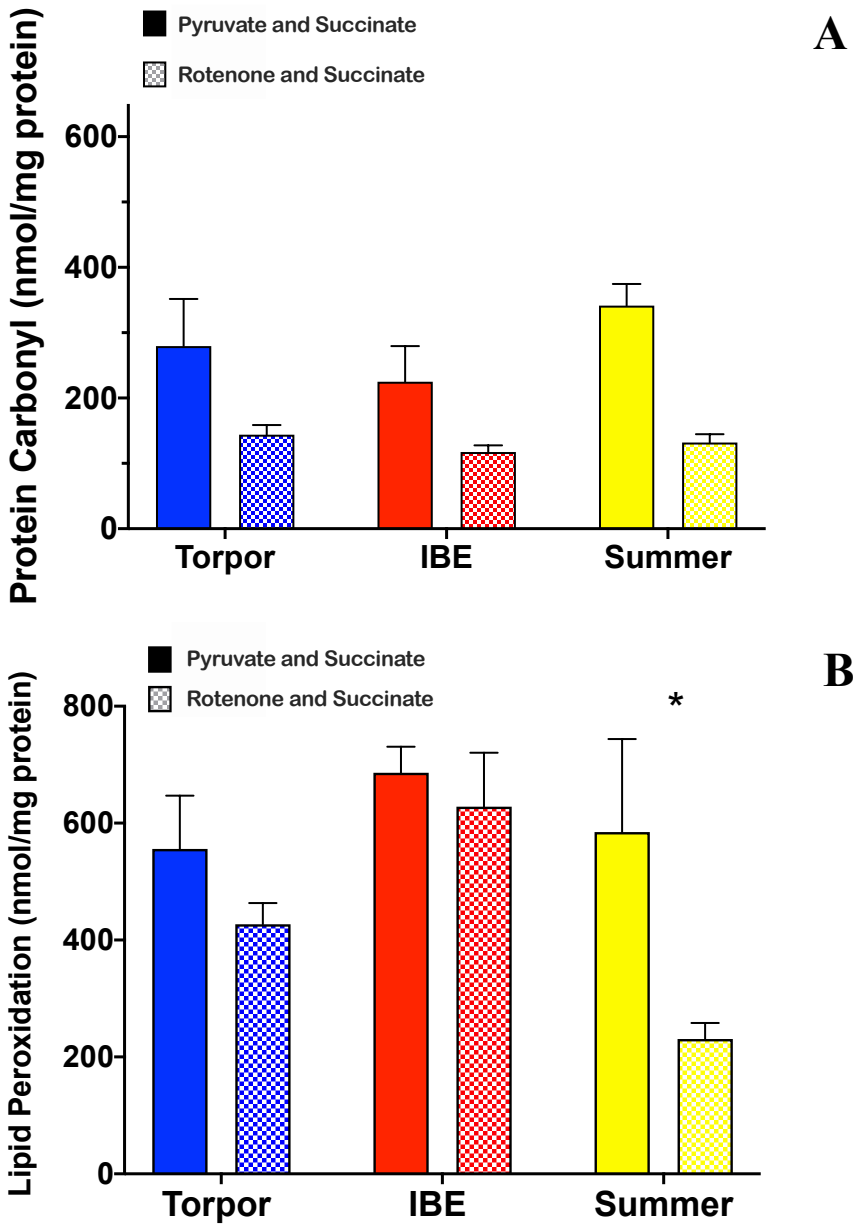

Figure 13. The effect of anoxia-reoxygenation on oxidative damage to mitochondrial proteins and lipids. Liver mitochondria isolated from torpor, IBE and summer ground squirrels, were supplied with either pyruvate and succinate (solid bars) or succinate alone (in the presence of rotenone; stippled bars) as an oxidative substrate. Protein carbonylation (A) and lipid peroxidation (B) were measured following five minutes of anoxia followed by reoxygenation. Asterisk indicates significant difference within summer and within succinate only mitochondria ($p \leq 0.05$; Repeated measures 2-way ANOVA, Bonferroni Post-hoc test). Mean ± SE, n=4 (all groups)

Chapter 4

4 Discussion

There is substantial evidence that hibernating animals avoid tissue damage typically associated with hypoxia-reoxygenation (34; 55; 60), an effect of the rapid and substantial changes of blood flow seen during arousal from torpor. Suppression of metabolism in hibernation may contribute to this avoidance of oxidative stress. Tolerance may be further enhanced with increased capacity to detoxify reactive oxygen species by antioxidants. This study aimed to:

1) compare markers of oxidative damage in torpor, IBE and summer in the thirteen-lined ground squirrel,

2) measure the functional effects of anoxia-reoxygenation on isolated mitochondrial respiration in these groups, and

3) determine if an antioxidant would mitigate any damage due to anoxia-reoxygenation.

I hypothesized that a mismatch between oxygen supply and demand (mimicking a major effect of ischemia-reperfusion injury) during hibernation would increase overall oxidative damage to tissue, but that this damage would be lower in the hibernation season than in summer TLGS. I further predicted that the metabolic suppression seen in isolated liver mitochondria from torpid TLGS would result in less oxidative damage following anoxia-reoxygenation compared with summer TLGS and rat mitochondria.

4.1 The effect of hibernation state on markers of ROS damage and antioxidant capacity in tissue

4.1.1 4.1.1 Lipid peroxidation

The general trend of lipid peroxidation suggests less tissue damage in summer than in the hibernation season, with more damage in IBE than torpor in some tissues (Figure 5A). Overall there is more variation in lipid damage among hibernation groups than either protein or nucleic acids (Figures 5B, 6).

In skeletal muscle (gastrocnemius), lipid peroxidation levels in TLGS are similar to those found in Daurian ground squirrels, *Spermophilus dauricus,* In the hibernation season, however, these levels increased 3-fold in TLGS (Figure 5A) and were much higher than Daurian ground squirrels (108). Differences between these species may relate to differences in antioxidant capacity between species, as Daurian ground squirrels reportedly have increased enzymatic antioxidant activity during hibernation (108). However, I did not observe an increase in TLGS total antioxidant capacity in TLGS during IBE or torpor states (Figure 7; see 4.1.4 below).

BAT and heart showed higher levels of lipid peroxidation in IBE than in either torpor or summer (Figure 5A). This finding contrasts with protein carbonylation data, in which neither BAT nor heart showed significant differences between hibernation states (Figure 5B). Additionally, the liver does not have significant differences in lipid peroxidation between hibernation states but did show differences in protein carbonylation. Differences among hibernation states may be due to functional and cellular differences among tissues.

Uncoupled mitochondrial respiration in BAT is required for thermogenesis during arousal from torpor to IBE (99). Reperfusion of BAT with high oxygen levels and the high metabolic rates in this tissue may increase the propensity for ROS production, leading to the increase in lipid damage seen in IBE. Further, in rats, BAT mitochondria have higher levels of polyunsaturated fatty acids (PUFAs) than liver, heart and brain mitochondria (14). If PUFA levels are also elevated in TLGS, it may contribute to the higher levels of damage.

Heart had 2-fold higher levels of lipid peroxidation in IBE than in torpor (Figure 5), the opposite pattern was observed in Daurian ground squirrels where IBE had lower levels of oxidative damage to lipids than torpor and summer (108). In TLGS, markers of myocardial ischemia (contraction bands, wavy fibers and hyper eosinophilia) are four-fold higher in IBE, when blood changes are most drastic, than summer (10). In non-hibernating rabbits, heart mitochondria produce higher ROS levels during the beginning of reperfusion than during ischemia (111). This pattern may be similar to the increase in blood flow during arousal in in TLGS, resulting in greater damage in IBE than torpor.

Small intestine also showed 2-fold higher levels of lipid peroxidation in IBE than torpor or summer (Figure 5A). This is consistent with past research in TLGS that suggests that intestinal mucosa is vulnerable to ischemia-reperfusion injury and showed higher levels of lipid peroxidation during the hibernation season than summer (17). My experiment further demonstrated that the reperfusion event of arousal corresponds with the higher lipid damage in IBE than torpor mitochondria.

Differences in antioxidant capacities could cause the difference in lipid peroxidation among hibernation states, but as discussed in section 4.1.4, I saw no changes in antioxidant capacity (Figure 7), suggesting that these differences are due to differential rates of ROS production. It is also possible that these differences are due to repair to damaged lipids during IBE. Lipid peroxidation can be stopped by the process of termination, in which two lipid peroxyl radicals react with each other to produce a non-radical species. However, this only happens when the concentration of lipid peroxyls is high. Damaged cellular membrane lipids can be repaired by thermodynamic resealing and by integral protein interactions with cytoskeleton components (9). Further, lipid repair likely occurs later in IBE before entrance into torpor as levels of damage in torpor are lower than IBE.

Overall, the results support my prediction that TLGS in IBE have more lipid oxidative damage than summer TLGS. Further, it reflects my prediction that lipid peroxidation would be greater than protein damage at the tissue level, because lipids are generally more susceptible to ROS damage than proteins. Additionally, hibernators

accumulate PUFA as the hibernation season approaches, and PUFA are very vulnerable to ROS damage, which may contribute to higher lipid peroxidation levels in the hibernation season (74).

4.1.2 Protein carbonylation

The general trend across all tissues suggests that protein damage is greater in the hibernation season (both IBE and torpor), when there is more variability in blood flow and oxygen supply compared with summer (Figure 5B). However, the changes in protein carbonylation were not as great as those in lipid peroxidation overall. Forebrain, BAT and liver protein carbonyl levels, in torpor and IBE (Figure 5B) were similar to values in torpid arctic ground squirrels, *Urocitellus parryii* (80). However, in summer euthermic TLGS, carbonyl levels in these tissues were five-fold lower than euthermic arctic ground squirrels (80). This discrepancy is likely due to experimental differences, as these euthermic arctic ground squirrels were held at 2 °C in the winter but did not hibernate. This lower ambient temperature would require higher metabolic rates to maintain euthermia, increasing electron flux through the ETS, generating more oxidative damage.

The gastrocnemius muscle is involved in shivering thermogenesis during arousal and suffers from atrophy over the hibernation season (110). In Golden-mantled ground squirrels there is approximately 25 % atrophy during hibernation in fast fiber type muscles, including plantaris and gastrocnemius (78). However, hibernators suffer less muscle atrophy than non-hibernating species, as muscle atrophy in mammalian hibernation is clearly lower than would be predicted from non-natural models of muscle disuse (49).

Lower summer protein carbonyls compared to hibernation support my hypothesis that arousal from torpor increases oxidative damage to tissue, likely due to the fluctuations in oxygen supply and demand. Higher protein damage of muscle and liver in torpor compared to IBE, was counter to my predictions that mitochondrial metabolic suppression during torpor in these tissues would mitigate oxidative damage during torpor. However, results overall suggest that metabolically active tissues suffer more from protein damage during torpor than less metabolically dynamic tissues such as small

intestine, and brain, and there are fewer tissues with significant differences between hibernation groups in protein damage.

Upregulated quality control and repair mechanisms may explain why proteins are less damaged than lipids in TLGS tissue. Cold exposure has long been associated with mitochondrial stress resistance in ground squirrels. For example, in neuronal pluripotent stem cells from TLGS, cold exposure alone, regardless of the hibernation state, results in upregulated gene expression specific for mitochondrial proteins and protein quality control (heat shock proteins, proteases, and proteinase inhibitors; 82). Further, as with mechanisms of lipid repair, it is likely that repair of removal of damaged proteins occurs after rewarming in IBE before reentry into torpor. Future studies should compare markers of oxidative damage over IBE and torpor. I predict that levels of oxidative damage would be lower at the end than at the beginning.

In TLGS, during arousal from torpor to IBE, there is a transient increase in heat shock protein mRNA. In BAT the expression of HSP90a increases 1.8-fold, and HSP60 increases 1.6-fold in WAT (89). During arousal, HSP90a may help stabilize cellular proteins and prevent protein aggregation. Likewise, HSP60 in WAT may serve similar functions during entrance into torpor, possibly by ensuring the maintenance of protein integrity during cooling. Further, HSP60 has been implicated in the maintenance of proper mitochondrial function and is associated with stabilization of cellular ROS levels (49). It is plausible that these mechanisms involved in protein quality control that are upregulated after cold exposure in isolated ground squirrel cells (82) are also upregulated in torpor and IBE. In my study, this effect could have mitigated some oxidative damage to proteins in mitochondria-dense tissues such as the liver.

4.1.3 DNA damage

Aside from the liver having more DNA damage (DNA abasic sites) than BAT in torpor, there were no significant differences among hibernation states (Figure 6). In TLGS, DNA damage may accumulate over the hibernation season, but shows no difference among hibernation states in the intestinal mucosa (39). My results also did not show significant differences in the proportion of DNA abasic sites among hibernation groups. Further,

they did not show any confounding effects of time in hibernation (time since first hibernation bout). Other forms of DNA damage, such as telomere shortening, occur during torpor in dormice (*Glis glis* and *Eliomys quercinus*; 79), so future studies should examine telomere dynamics in TLGS within the hibernation season.

My results do not support my preliminary hypothesis that the hibernating groups would accumulate more DNA damage than summer TLGS. However, I did predict that DNA would exhibit less oxidative damage than either lipids or proteins, given its stronger molecular structure and the higher rates of DNA repair. Specifically, base excision repair recognizes damage to one or a few bases and is the primary mammalian mechanism for repairing abasic sites.

During torpor in TLGS, the genome undergoes structural modifications that render DNA largely inaccessible to transcription (102) and likely limit access of ROS to DNA. These genomic alterations decrease during IBE when most DNA repair is thought to occur (8). It is possible that DNA damage is lower in torpor than IBE, but that repair rates are higher in IBE than torpor, which may explain why we see no variation in DNA damage between states.

4.1.4 Total Antioxidant Capacity

Aside from higher levels of total antioxidant capacity (TAC) in summer kidney (Figure 7), TAC did not change among hibernation states in TLGS. These observations support the literature, which generally suggests that intracellular antioxidant enzymes do not vary among hibernation groups in TLGS. For example, in liver, heart, and brain tissue, superoxide dismutase (both Mn and CuZn), glutathione peroxidase, and glutathione reductase showed no difference in protein expression or activity between hibernating and summer TLGS, although catalase showed variable increases in activity between tissues - it was higher in heart and brain of hibernating squirrels, but lower in liver (84). Because antioxidants detoxify ROS and prevent oxidative damage, any differences in damage among hibernation states found in my study are likely due to differences in ROS production rates. However, some non-enzymatic and extracellular antioxidants may vary among hibernation states. For example, ascorbate levels in blood plasma vary during

hibernation, decreasing during arousal, suggesting increased tissue uptake during periods of potentially high oxidative stress (32).

In arctic ground squirrels, ascorbate clearance from plasma to tissues is associated with peak oxygen consumption during arousal, which coincides with reperfusion of central organs (heart, lungs, liver), even when body temperature is still low (103). During arousal, when oxygen consumption is highest, and reperfusion damage is expected to be highest, plasma ascorbate levels progressively decrease to levels similar to summer ground squirrels, suggesting that elevated concentrations of plasma ascorbate in the hibernation season may protect metabolically active tissues from increased oxidative stress (31). If there was a significant pool of non-enzymatic antioxidants in the blood, I would not have detected them using my TAC assay. Further, once taken up by the tissues in IBE, ROS may quickly quench ascorbate, and then would not be detectable. Future studies should measure ascorbate clearance from plasma in TLGS, and ascorbate accumulation in metabolically demanding tissues such as liver, and BAT during torpor, arousal and IBE.

4.2 Impacts of anoxia-reoxygenation on mitochondrial respiration, and mitigation by an exogenous antioxidant

4.2.1 The effect of anoxia-reoxygenation on mitochondrial performance

Isolated liver mitochondria were subjected to five minutes of anoxia followed by reoxygenation to simulate *in vitro* the effects of low perfusion during torpor followed by reperfusion during IBE. I used anoxia to ensure consistent oxygen levels and because it is difficult to maintain hypoxia in Oxygraph chambers. Further, isolated mitochondria can function normally under very low oxygen levels, as oxygen dependence of mitochondrial respiration remains constant until less than 1 % air saturation (43). I used five minutes of anoxia because previous work found no significant differences in the effect of 5 minutes compared with 30 minutes of anoxia, followed by reoxygenation (46).

Maximal ADP-stimulated respiration rates of isolated liver mitochondria were consistent with previous literature on TLGS following anoxia-reoxygenation (46). However, my ST3 respiration rates were 20 % more suppressed in torpor than previous

work - I found that in torpor respiration rates were reduced by 50 % when both pyruvate and succinate were supplied as substrates (Figure 8A) whereas previous work found suppression of only 30 % (46). However, I found similar metabolic suppression in torpor when only a complex II-linked substrate (succinate with rotenone) was oxidized (Figure 8B), similar to previous studies (65). ST4 rates are overall similar to the recent work, except my ST4 rates were 20 % higher before anoxia-reoxygenation in summer TLGS (65; 46). These apparent small discrepancies are likely due to the variability in mitochondria isolation techniques among individual researchers.

In isolated rat liver mitochondria oxidative phosphorylation performance declined more following anoxia-reoxygenation compared with TLGS. Anoxia-reoxygenation decreased ST3 respiration rate in rats by 65 % (with both succinate and pyruvate as substrates) and 69 % (using succinate as substrate with complex I inhibited by rotenone) of initial values, compared with 10-16 % for torpor, 30-33 % for IBE and 32-38 % for summer depending on the substrates used (Figure 8). This supports previous observations that hibernator tissues are inherently more resistant to ischemia-reperfusion injury, even during the summer (60). Additionally, tolerance to anoxia-reoxygenation is likely not exclusively an effect of inherently lower mitochondrial respiration rates; rat liver mitochondria had lower ST3 rates than TLGS but showed greater decreases in mitochondrial performance after reoxygenation (Figure 8).

However, ST4 respiration rates were lower in rats than in TLGS and, unlike TLGS, were not affected significantly by anoxia-reoxygenation (Figure 9). The lack of increase in ST4 suggests that rat membranes were not as damaged by anoxia-reoxygenation as the ground squirrels, perhaps because rats tend to have fewer PUFAs in isolated liver mitochondria than TLGS, and PUFA are more susceptible to oxidative damage (74). The higher PUFA in hibernators may have evolved to permit maintained membrane fluidity at varying temperatures but comes at the expense of higher susceptibility to lipid peroxidation.

Liver mitochondria from torpid ground squirrels maintained oxidative phosphorylation performance better after anoxia-reoxygenation than either IBE or

summer TLGS mitochondria, consistent with previous reports (46). Anoxia-reoxygenation decreased the ST3 respiration in all groups, but torpor was affected the least, falling by 10-16 % of initial values, compared with 30 % for IBE and 32-38 % for summer (Figure 8). Leak (ST4) respiration rates increased 13-20 % in summer TLGS (Figures 9). Overall there is less damage during torpor when mitochondrial metabolism is suppressed.

Less oxidative damage during torpor may have resulted from lower accumulation of succinate during anoxia and lessened oxygen availability, leading to less RET generated ROS production (Figure 2B). The oxidation of succinate by complex II during reoxygenation can saturate ubiquinol, and is one of the primary driving forces of RET, leading to increased ROS production from complex I. The Staples lab has previously demonstrated that liver mitochondrial oxidation of succinate and pyruvate is reversibly suppressed during torpor (72, 22). Succinyl-CoA ligase catalyzes the conversion of succinyl-CoA to succinate in the TCA cycle and is a potential site of regulation of succinate accumulation, as phosphorylation increases activity of the enzyme (65). Phosphorylation of succinyl-CoA ligase increases by 4.6-fold in IBE compared to torpor (67), suggesting lower rates of succinate production in torpor. The suppression of mitochondrial succinate metabolism in torpor, and its slow reversal in arousal, likely minimize ROS production and oxidative damage during torpor compared to IBE. In TLGS, succinate levels are 3.5- and 2.7-fold higher in summer livers compared with late torpor and re-entering torpor livers (94). However, no succinate data exist for IBE, where ROS production by RET is most likely. Future studies should measure succinate levels in isolated liver mitochondria using gas chromatography to compare succinate accumulation within the mitochondria between torpor and IBE.

Lowered mitochondrial metabolism in torpor may also contribute to lessened ROS generation rates, due to suppressed succinate oxidation through complex II and suppressed CoQ oxidation through complex I. In RET, accumulated succinate is first metabolized through complex II, reducing ubiquinone. Liver mitochondria isolated from torpid TLGS have lower maximal rates of succinate dehydrogenase activities than summer and interbout euthermic individuals (2). This suppression of activity is reversible

within hours of arousal to IBE (2). Phosphorylation of the flavoprotein of complex II increases by 4.6-fold during IBE compared to torpor. Lower activity of complex II during torpor may account for lowered ROS damage, as accumulated succinate can be oxidized when succinate dehydrogenase is active and can initiate RET that leads to increases in ROS production. Further, in RET, the reduced ubiquinol is oxidized by complex I, which is the site of most ROS production through RET. While less suppressed during torpor compared to complex II, complex-I activity is still lower during torpor (65). Phosphorylation of the 75-kDa subunit of complex I is 1.5-fold greater in torpor than IBE, and removal of phosphate groups results in complete reversal of complex I suppression (67). Lowered complex I activity during torpor most likely lessens ROS production at ubiquinol oxidation sites of complex I. Future studies should inhibit complex II with malonate to prevent succinate from entering the ETS and measure changes in levels of ROS production under anoxic conditions.

In addition to hibernation state, performance after anoxia-reoxygenation is affected by ETS complex activity, especially in summer TLGS. For example, ST3 rates were lower following anoxia-reoxygenation when complex I was active in summer (38 % compared to 32 % for the complex II substrate; Figure 8). Leak (ST4) respiration rates were generally higher when complex I was active, such as in summer (20 % compared to 13 %) (Figures 9).

These results indicate that mitochondria isolated from TLGS maintain bioenergetic capacity better than non-hibernating rats. Further, within TLGS, mitochondria isolated from torpor maintain bioenergetic integrity better than those from summer and IBE animals. Finally, ETS complex I is a significant contributor to anoxia-reoxygenation damage in isolated mitochondria.

4.2.2 Effect of exogenous antioxidant on anoxia-reoxygenated mitochondria

The addition of ascorbate mitigated the decline in ST3 (Figure 10) and increase in ST4 (Figure 11) in both complex I-active (Figure 10A; Figure 11A) and complex I-inhibited (Figure 10B; Figure 11B) liver mitochondria from IBE and torpid TLGSs. In ST3 with

ascorbate treatment, IBE and torpor were significantly higher post anoxia reoxygenation than without ascorbate. This apparent protective effect was further augmented when complex I was inhibited. With ascorbate, torpor showed less increases in ST4 compared to IBE (Figure 11). The mitigating effects of ascorbate suggest that the functional changes following anoxia-reoxygenation were caused by ROS-mediated damage.

Ascorbate is a water-soluble antioxidant that cannot penetrate the hydrophilic inner mitochondrial membrane, so it likely helped detoxify ROS released into the intermembrane space by ETS complex III. Complex-I releases superoxide to the mitochondrial matrix, which would not be accessible to ascorbate. My data are consistent with these actions of ascorbate; when both complexes I and II are active ascorbate would quench ROS released by complex III. However, ascorbate would not be able to directly quench ROS generated through RET into the matrix by complex I. Ascorbate could still indirectly detoxify ROS *in vivo* by replenishing vitamin E, which can diffuse into the matrix, but this would take longer and would likely be insufficient to reduce immediate reperfusion damage to mitochondrial respiration. On the other hand, when complex I is inhibited (using rotenone with succinate as complex II substrate), ascorbate would quench ROS released by complex III, likely mitigating most damage.

In summary, differential tolerance to anoxia-reoxygenation in this study is likely related to ROS production, especially by ETS complex I activity. To clarify this data set, future experiments should determine the effects of ascorbate in mitochondria isolated from euthermic, summer TLGS and rats. I had planned these experiments for the spring and early summer of 2020 but the restrictions due to the COVID-19 pandemic made them impractical.

4.3 Effect of anoxia-reoxygenation on markers of ROS damage to isolated mitochondria

4.3.1 Mitochondrial Protein Carbonylation

Freshly isolated liver mitochondria did not differ in protein carbonyl levels among summer and hibernation states (Figure 12A). Protein carbonyl levels in isolated liver mitochondria of TLGS are approximately 3-fold higher than values of isolated rat liver

mitochondria reported in literature (28). This discrepancy may be due to the method of detection, as the previous study used an ELISA method that is more sensitive and discriminatory than my DNPH-derived colorimetric assay. However, my protocol did result in measurable protein carbonylation. In fact, isolated liver mitochondria that underwent anoxia-reoxygenation had at least 8-fold higher protein damage than freshly isolated mitochondria. This result suggests that anoxia-reoxygenation caused significant damage to mitochondrial proteins. However, it would have been best to compare the anoxia-reoxygenation condition with freshly isolated mitochondria had not undergone *in vitro* oxidative phosphorylation under normoxic conditions (i.e. without exposure to anoxia). I had planned to make these comparisons but was prevented by COVID-19 restrictions on research activities.

Protein carbonyl levels of mitochondria using both complex-I and II substrates appeared higher but did not differ significantly when complex-I was inhibited by rotenone (Figure 13B). These findings again suggest that RET may be contributing to mitochondrial protein oxidative damage, in addition to the functional effects of ST3 mitochondria.

4.3.2 Mitochondrial Lipid Peroxidation

As with protein carbonylation, freshly isolated liver mitochondria did not differ in lipid peroxidation among hibernation groups (Figure 12B). Anoxia-reoxygenation did not drastically increase lipid peroxidation compared with freshly isolated mitochondria (Figure 12B, 13A). This result reflects some of the functional effects of anoxia-reoxygenation on mitochondrial respiration. The increase in ST4 (membrane proton leak) was not proportional to the decrease in ST3 (maximal respiration, dependent on protein function) observed after anoxia-reoxygenation. Together, these results suggest that ROS caused more damage to mitochondrial proteins (which catalyze oxidative phosphorylation) than lipids (which act as the principle barrier to proton leak). This result in isolated mitochondria is opposite to the pattern found in tissues, and counter to my hypothesis which led me to predict greater lipid damage than protein damage.

Higher protein damage in isolated liver mitochondria is likely due to several factors including lipid/protein composition, lipid remodeling, and lack of protein quality control in isolated mitochondria. As briefly alluded to in 4.1.1, lipid abundance is higher in whole tissue than mitochondria; tissues contain both membrane phospholipids and storage triglycerides, whereas lipids within mitochondria are restricted predominantly membrane phospholipids. Further, the inner-mitochondrial membrane is composed of 80 % proteins, compared with only 50 % for most other membranes (54). Therefore, the higher levels of protein damage than lipid damage in mitochondria may simply reflect the relatively higher levels of proteins in close proximity to ROS produced in the ETS.

It is also possible that the relatively lower lipid damage in isolated mitochondria following anoxia-reoxygenation is due to lipid remodeling that occurs during hibernation. For example, in isolated TLGS liver mitochondria phospholipids, palmitoleic acid (a monounsaturated fatty acid; MUFA; 16:1) is two-fold higher in IBE than torpor. Although 16:1 accounts for only 1.5 % of total phospholipids, its levels correlated strongly with ST3 respiration. An increase in 16:1 may help to reduce oxidative damage to mitochondrial membranes by replacing PUFA with a MUFA (3). Lipid remodeling may protect mitochondrial lipids from ROS damage and explain lessened markers of oxidative damage compared to proteins.

Protein quality control in whole tissue is likely upregulated following cold exposure by heat shock proteins (HSPs), proteases, and proteinase inhibitors. HSP70 is a primary mitochondrial chaperone upregulated at the beginning of torpor (18). Despite being a mitochondrial chaperone, the protein is synthesized in the cytosol and must be imported into the mitochondrial matrix (30). My results suggest that such mechanisms require at least intact cells to protect against anoxia-reoxygenation damage.

Additionally, as with protein damage, lipid damage tended to be slightly higher when complex I was active (Figure 13). This further suggests that RET contributes excess ROS in anoxia-reoxygenation leading to oxidative damage. In conclusion, markers of oxidative damage in isolated liver mitochondria are higher after anoxia-reoxygenation, more elevated when complex-I is active, and are higher in protein than in lipids. Future

studies should also compare mitochondrial DNA damage between hibernation groups, with different oxidative substrates post anoxia-reoxygenation. Again, my original plans for conducting these experiments during the spring/summer of 2020 were curtailed due to the COVID-19 shut down.

4.4 Oxidative damage and tolerance in hibernation

Ischemia-reperfusion injury occurs when physiological mechanisms are disrupted by fluctuations in oxygen availability due to a transient cessation in blood flow. My study demonstrated that hibernating TLGS accrue oxidative damage to tissues like those seen in ischemia-reperfusion injury. Moreover, I demonstrate that isolated liver mitochondria subjected to anoxia-reoxygenation also sustain such damage, which correspond to changes in mitochondrial respiration. The damage to mitochondria, however, differ according to hibernation state and oxidative pathway.

Ischemia-reperfusion likely causes oxidative damage by several mechanisms as discussed below. However, hibernating mammals exhibit an innate physiological ability to withstand the dramatic fluctuations in blood flow that occur during hibernation and are experimental models of resistance to ischemia-reperfusion injury (7). I have demonstrated that TLGS mitochondria maintain mitochondrial function after anoxia-reoxygenation better than non-hibernating rats. Mechanisms of anoxia-reoxygenation tolerance likely help mitigate the oxidative damage observed in my study.

4.4.1 Oxidative damage during oxidative phosphorylation

I observed less oxidative damage when metabolism was suppressed in hibernation compared to summer in tissue and in torpor compared to all states in ST3 metabolism. Previous studies have also found that during hibernation in TLGS, changes to oxidative phosphorylation by active suppression of metabolism and passive thermal effects, affect ROS production in torpor and IBE (13). ROS production rates proportionally increase with elevated proton motive force and available oxygen. Due to mass action effects, high proton motive force slows electron transfer through the ETS, which leads to increased electron leakage from ETS complexes and reduction of more O_2 to ROS. Molecular oxygen is very electronegative, and so higher local O_2 concentrations more readily

accepts electrons than ETS proteins, further increasing the potential ROS production. ROS production in IR injury likely comes from the accumulation of succinate during ischemia that then drives mitochondrial ROS production by reverse electron transport at complex I during reperfusion (75).

Small ubiquitin-related modifiers (SUMO) have been implicated in ischemia preconditioning. Covalent binding of SUMOs to lysine residues on target proteins modify their function. These post-translational modifications (PTMs) are upregulated during torpor in TLGS in many organs, including the liver (58). Decreases in the levels of specific miRNAs (from the MiR-200 and MiR-182 families) in TLGS brain occurs during torpor and indirectly increases global SUMOylation, providing tolerance to ischemia (58). Future studies should measure SUMO post-translational modifications before and during hibernation, with markers of oxidative damage, and ROS production, to study correlative effects.

Several other PTMs, including phosphorylation, acetylation, and succinylation, play complex roles in regulation of mitochondrial metabolism (48). Differential PTMs of mitochondrial enzymes are known to correspond with metabolic suppression that likely reduce oxidative damage. For example, complex I is 50 % more phosphorylated during torpor than IBE (66), corresponding with reduced activity (65). Further, the flavoprotein subunit of complex II has higher phosphorylation in IBE than torpor (66), corresponding with reduced activity (65). Together this suppression of ETS complexes could reduce RET by preventing accumulated succinate from reducing coenzyme Q, and the subsequent reduction of complex I. Such mechanisms could account for the lower damage to torpor mitochondria found in this study when complex I was not inhibited.

4.4.2 Super-complexes

It is well established that ETS complexes can assemble within the inner mitochondrial membrane into higher-order structures known as super-complexes (1). These super-complexes can increase respiration efficiency and reduce ROS production (67), so it is possible that changes in super-complex assembly among hibernation states accounts for the differences that I found. Cardiolipin is a phospholipid that stabilizes super-complexes

(85). Cardiolipin content of liver mitochondria increases by 50 % in arctic ground squirrels during hibernation compared to the summer (53). Loss of cardiolipin during ischemia increases ROS production from complex III (20). However, an earlier study found no change in cardiolipin content of liver mitochondria between IBE and torpor TLGS (22).

Differential tolerance to anoxia-reoxygenation is best explained as a function of ROS production in my study. If super-complex stability is truly enhanced in hibernators during the winter compared to summer, ROS production may also be reduced, protecting against anoxia.

4.4.3 Ischemic Preconditioning

As previously discussed, in humans, ischemic events are considered to have "bimodal" effects, where brief bouts of ischemia are protective, and mount ischemia preconditioning cellular mechanisms, whereas long bouts lead to damage. Before hibernation, TLGS undergo "test drops," during which they metabolically cycle through states similar to torpor and IBE, but last less than two days, with body temperatures falling only to around 20 °C (91). Researchers have speculated that these test-drops establish a protective phenotype similar to ischemia preconditioning, which may help TLGS to reduce oxidative damage that occurs during hibernation (91).

4.4.4 Antioxidants

My study showed no differences in tissue TAC between hibernation states, leading me to suspect any differences in tissues are likely due to changes in ROS production. However, other antioxidants may contribute additional roles of protection that were not detected in this study. A comprehensive study of plasma metabolites in TLGS revealed an increase in plasma cysteine and cystathionine during late torpor (29). Plasma cysteine is a precursor of glutathione, an important component to antioxidant systems within the mitochondrial matrix. In hibernating Syrian hamsters, glutathione peroxidase 4 is the only isoenzyme that can detoxify cell membrane polyunsaturated phospholipid hydroperoxides and its activity is essential to lower lipid peroxidation levels following anoxia-reoxygenation (35). However, in TLGS activity of glutathione peroxidase and glutathione reductase are

not broadly upregulated during hibernation (83). Future studies should compare levels of reduced and oxidized glutathione as a measure of oxidative stress among hibernation states.

Cysteine and cystathionine are also substrates for cystathionine beta synthetase (CBS) that produces hydrogen sulfide (H_2S). H_2S is thought to be an important regulator of ROS production through its inhibition of complex IV in mitochondria. The administration of H_2S during reperfusion of ischemic mouse hearts correlates with higher ST3 in mitochondria isolated from these hearts (38). Since H_2S binds to complex IV with a low affinity, its inhibitory effect occurs predominantly during hypoxia because it is rapidly oxidized as O_2 levels climb (87).

In TLGS tissues, H_2S levels appear to fluctuate seasonally, being higher during the hibernation season than in summer (50). Further, in TLGS, H_2S inhibits succinate-fueled mitochondrial respiration, and mitochondria have a higher sensitivity to H_2S inhibition during torpor than IBE or summer (50). H_2S, therefore, may be a plausible mechanism for controlling oxidative damage in hibernators, especially during torpor.

4.5 Discussion summary

Various physiological changes occur during hibernation in TLGS that may confer tolerance to ischemia-reperfusion injury to tissue, or anoxia-reoxygenation to mitochondria. My primary goal was to compare the effects of rapid changes in available oxygen, due to blood flow fluctuations, on oxidative damage among TLGS hibernation states, and to determine the functional impact of anoxia reoxygenation on isolated liver mitochondrial respiration. My data suggest that TLGS experience ROS damage during the hibernation season in tissue, but that functional consequences of anoxia-reoxygenation are attenuated at the mitochondrial level during hibernation and can further be mitigated with the addition of an exogenous antioxidant.

Chapter 5

5 Conclusions and future directions

The goal was to determine whether mitochondrial metabolic plasticity during hibernation, especially suppression during torpor, could partly explain ischemia-reperfusion tolerance during hibernation. My findings demonstrate greater anoxia-reoxygenation tolerance in mitochondria isolated from ground squirrels than non-hibernating rats. These results also suggest that anoxia-reoxygenation tolerance is greater in ground squirrels during the hibernation season, especially torpor, compared to summer squirrels. This mitochondrial anoxia-reoxygenation tolerance likely contributes to documented ischemia-reperfusion tolerance in hibernators, despite my measured increases in oxidative damage of hibernating tissues.

Anoxia-reoxygenation tolerance in isolated mitochondria reflects mitochondrial oxidative damage assays, as I measured lipid peroxidation markers and protein carbonylation in isolated mitochondria and found no differences between freshly isolated groups. However, isolated mitochondria that underwent anoxia-reoxygenation showed higher levels of damage. Future studies should utilize fluorescent probes developed for the Oxygraph to measure reactive oxygen species production and oxygen consumption during anoxia-reoxygenation in these groups to correlate decreased ROS production and metabolic suppression. Additionally, oxidative damage differed depending on ETS complex activity. Further study with fluorescent probes should also measure differences in ROS production dependent on complex activity.

Other physiological changes related to metabolic suppression may confer anoxia-reoxygenation tolerance during hibernation. For example, hydrogen sulfide levels fluctuate with metabolic changes and are also known to have antioxidant properties (50). Additionally, post-translational modifications are known to confer hypoxia tolerance during metabolic suppression while also possibly contributing to metabolic regulation during hibernation (e.g. Phosphorylation (65) and SUMOs (57)). More work should compare levels of H_2S and post-transitional modifications on mitochondrial metabolic regulation and reactive oxygen species production among hibernation states. Finally,

mitochondrial super-complex formations may differ depending on metabolic activity and plasticity and could manipulate ROS production and damage, altering function. Future work should incorporate and compare ETS dynamics with ROS production among hibernation states.

My study compares oxidative damage among hibernation states at the tissue and mitochondrial level and further demonstrates functional resistance to anoxia-reoxygenation in hibernating mitochondria. Overall, my data suggests that suppressed metabolism during hibernation is protective against changes in oxygen availability. Markers of oxidative damage provide information on the physiological consequences of ROS, but direct measurements of ROS production would increase understanding of ROS dynamics during hibernation. Future studies should aim to repeat a study similar to my design, while simultaneously measuring mitochondrial ROS production among hibernation states.

References

1. **Acín-Pérez, R., Fernández-Silva, P., Peleato, M.L., Pérez-Martos, A. and Enriquez, J.A.** (2008). Respiratory active mitochondrial supercomplexes. *Molecular cell* **32**, 529–539.
2. **Armstrong, C. and Staples, J.F. (**2010). The role of succinate dehydrogenase and oxaloacetate in metabolic suppression during hibernation and arousal. *Journal of Comparative Physiology B*, **180**, 775–783.
3. **Armstrong, C., Thomas, R. H., Price, E. R., Guglielmo, C. G. and Staples, J. F.** (2011). Remodeling Mitochondrial Membranes during Arousal from Hibernation. *Physiological and Biochemical Zoology* **84**, 438–449.
4. **Armitage, K. B. and Shulenberger, E.** (1972). Evidence for circannual metabolic cycle in Citellus tridecemlineatus, a hibernator. *Comparative Biochemistry Physiology Part A: Physiology* **42**, 667–688.
5. **Bech, C., Abe, A. S., Fleng Steffensen, J., Berger, M., Eduardo, J. and Bicudo, P. W.** (1997) Torpor in three species of brazilian hummingbirds under semi-natural conditions. *The Condor* **99**,780–78X.
6. **Becker, L. B., Vanden Hoek, T. L., Shao, Z., Schumacker, P. T., Shao, Z.-H., Li, C.-Q. and Schumacker Genera, P. T.** (1999). Generation of superoxide in cardiomyocytes during ischemia before reperfusion. *American Journal of Physiology-Heart and Circulatory Physiology*. **277**, H2240–H2246.
7. **Bhowmick, S. and Drew, K. L.** (2019). Mechanisms of innate preconditioning towards ischemia/anoxia tolerance: Lessons from mammalian hibernators HHS *Conditioning Medicine* **2**, 134.
8. **Biggar, Y. and Storey, K. B.** (2014). Global DNA modifications suppress transcription in brown adipose tissue during hibernation. *Cryobiology* **62**, 333–338.
9. **Blazek, A. D., Paleo, B. J., Weisleder, N., Blazek, A. D. and Paleo, B. J.** (2015). Plasma Membrane Repair: A Central Process for Maintaining Cellular Homeostasis. *Physiology* **30**, 438–448.
10. **Bonis, A., Anderson, · Leah, Talhouarne, G., Schueller, E., Unke, J., Krus, C., Stokka, J., Koepke, A., Lehrer, B., Schuh, · Anthony, et al.** (2019). Cardiovascular resistance to thrombosis in 13-lined ground squirrels. *Journal of Comparative Physiology and Biochemistry* **189**, 167–177.
11. **Brown, J. C. L., Chung, D. J., Belgrave, K. R. and Staples, J. F.** (2012). Mitochondrial metabolic suppression and reactive oxygen species production in liver and skeletal muscle of hibernating thirteen-lined ground squirrels. *American Journal of Physiology- Regulatory, Integrative and Comparative Physiology* **302**, 15–28.
12. **Brown, J. C. L. and Staples, J.F.** (2014). Substrate-specific changes in mitochondrial respiration in skeletal and cardiac muscle of hibernating thirteen-lined ground squirrels. *Journal of Comparative Physiology B.* **184**, 401–414.
13. **Brown, J. C. L. and Staples, J. F.** (2011). Mitochondrial Metabolic Suppression in Fasting and Daily Torpor: Consequences for Reactive Oxygen Species Production. *Physiological and Biochemical Zoology* **84**, 467–480.

14. **Buzadžić, B., Spasić, M., Saičić, Z. S., Radojičić, R., Petrović, V. M., & Halliwell, B.** (1990). Antioxidant defenses in the ground squirrel Citellus citellus. The effect of hibernation. *Free Radical Biology and Medicine.* **9**, 407–413.
15. **Cannon, B. and Linberg, O.** (1979) Mitochondria from brown adipose tissue: Isolation and properties. In *Methods in enzymology*. **8**, 65–78.
16. **Cannon, B. and Nedergaard, J.** (2004). Brown Adipose Tissue: Function and Physiological Significance. *Physiological Reviews* **84**, 277–359.
17. **Carey, H. V., Frank, C. L. and Seifert, J. P.** (2000). Hibernation induces oxidative stress and activation of NF-κB in ground squirrel intestine. *Journal of Comparative Physiology - B Biochemistry* **170**, 551–559.
18. **Carey, H.V., Lindell, S., Fleck, C. and Southard, J**. (2002). Hibernation induces superior cold storage ability in liver. In *Gastroenterology* **122**, A354–A354.
19. **Chayama, Y., Ando, L., Tamura, Y., Miura, M. and Yamaguchi, Y.** (2016). Decreases in body temperature and body mass constitute pre-hibernation remodeling in the Syrian golden hamster, a facultative mammalian hibernator. *Royal Society open science*. **3**, 160002.
20. **Chen, Q. and Lesnefsky, E. J.** (2006). Depletion of cardiolipin and cytochrome c during ischemia increases hydrogen peroxide production from the electron transport chain. *Free Radical Biology and Medicine*. **40**, 976–982.
21. **Chouchani, E. T., Kazak, L., Jedrychowski, M. P., Lu, G. Z., Erickson, B. K., Szpyt, J., Pierce, K. A., Laznik-Bogoslavski, D., Vetrivelan, R., Clish, C. B., et al.** (2016). Mitochondrial ROS regulate thermogenic energy expenditure and sulfenylation of UCP1. *Nature* **532**, 112–116.
22. **Chung, D., Lloyd, G. P., Thomas, R. H., Guglielmo, C. G. and Staples, J. F.** (2011). Mitochondrial respiration and succinate dehydrogenase are suppressed early during entrance into a hibernation bout, but membrane remodeling is only transient. *Journal of Comparative Physiology B* **181**, 699–711.
23. **Cooper, C. E., Kortner, G., Brigham, M. and Geiser, F.** (2010). Body temperature and activity patterns of free-living laughing Kookaburras: the largest Kingfisher is heterothermic. *The Condor* **110**, 110–115.
24. **Cooper, C. E. and Brown, G. C.** (2008). The inhibition of mitochondrial cytochrome oxidase by the gases carbon monoxide, nitric oxide, hydrogen cyanide and hydrogen sulfide: chemical mechanism and physiological significance. *Journal of Bioenergetics and Biomembranes* **40**, 533.
25. **Criddle, S.** (1939) The thirteen-striped ground squirrel in Manitoba. *Canadian field naturalist*. **53**, 1–6.
26. **Curtis, J. M., Hahn, W. S., Long, E. K., Burrill, J. S., Arriaga, E. A., & Bernlohr, D. A.** (2012) Protein carbonylation and metabolic control systems. *Trends in endocrinology and metabolism: TEM*, **23**, 399–406.
27. **Dausmann, K. H., Glos, J., Ganzhorn, J. U. and Heldmaier, G.** (2004). Hibernation in a tropical primate. *Nature* **429**, 825–826.
28. **Davies, S.M., Poljak, A., Duncan, M.W., Smythe, G.A. and Murphy, M.P.** (2001) Measurements of protein carbonyls, ortho-and meta-tyrosine and oxidative phosphorylation complex activity in mitochondria from young and old rats. *Free Radical Biology and Medicine*. **31**, 181–190.

29. **D'alessandro, A., Nemkov, T., Bogren, L. K., Martin, S. L. and Hansen, K. C.** (2016). Comfortably Numb and Back: Plasma Metabolomics Reveals Biochemical Adaptations in the Hibernating 13-Lined Ground Squirrel. *Journal of proteome research* **16**, 958–969.
30. **Deocaris, C. C., Kaul, S. C. and Wadhwa, R.** (2006). On the brotherhood of the mitochondrial chaperones mortalin and heat shock protein 60. *Cell stress & chaperones*. **11**, 116.
31. **Drew, K. L., Tøien, Ø., Rivera, P. M., Smith, M.A., Perry, G., Rice, M.E.** (2002) Role of the antioxidant ascorbate in hibernation and warming from hibernation. *Comparative Biochemistry and Physiology* **133**, 483–492.
32. **Drew, K. L., Osborne, P. G., Frerichs, K. U., Hu, Y., Koren, R. E., Hallenbeck, J. M. and Rice, M. E.** (1999) Ascorbate and glutathione regulation in hibernating ground squirrels. *Brain research.* **851**: 1–8.
33. **Drew, K. L., Rice, M. E., Kuhn, T. B. and Smith, M. A.** (2001). Neuroprotective adaptations in hibernation: therapeutic implications for ischemia-reperfusion, traumatic brain injury and neurodegenerative diseases. *Free Radical Biology and Medicine*. **31**, 563–573.
34. **Drew, K. L., Zuckerman, J., Bogren, L. and Jinka, T. R.** (2013) Hibernation: A Natural Model of Tolerance to Cerebral Ischemia/Reperfusion. In *Innate tolerance in the CNS*. 37–50.
35. **Eleftheriadis, T., Pissas, G., Liakopoulos, V. and Stefanidis, I.** (2019) Factors that may protect the native hibernator syrian hamster renal tubular epithelial cells from ferroptosis due to warm anoxia-reoxygenation. *Biology*, **8**, 22.
36. **Else, P. L. and Hulbert, A. J.** (1981). Comparison of the mammal machine and the reptile machine: energy production. *American Journal of Physiology-Regulatory, Integrative and Comparative Physiology* **240**, R3-9.
37. **Else, P. L. and Hulbert, A. J.** (1985). An allometric comparison of the mitochondria of mammalian and reptilian tissues: the implications for the evolution of endothermy. *Journal of Comparative Physiology* **156**, 3–11.
38. **Elrod, J.W., Calvert, J.W., Morrison, J., Doeller, J.E., Kraus, D.W., Tao, L., Jiao, X., Scalia, R., Kiss, L., Szabo, C. and Kimura, H.** (2007). Hydrogen sulfide attenuates myocardial ischemia-reperfusion injury by preservation of mitochondrial function. *Proceedings of the National Academy of Sciences*, **104**, 15560–15565.
39. **Fleck, C. C. and Carey, H. V** (2005). Modulation of apoptotic pathways in intestinal mucosa during hibernation. *American Journal of Physiology-Regulatory, Integrative and Comparative Physiology* **289**, 586–595.
40. **Galli G. L. J., Lau G. Y., Richards J. G.** (2013) Beating oxygen: chronic anoxia exposure reduces mitochondrial F1FO-ATPase activity in turtle (Trachemys scripta) heart. *Journal of Experimental Biology* **216**, 3283–3293.
41. **Gear, A.R.L., and Bednarek, J.M.** (1972) Direct counting and sizing of mitochondria in solution. *Journal of Cellular Biology* **52**, 325–345.
42. **Geiser, F.** (1998). Evolution of daily torpor and hibernation in birds and mammals: importance of body size. *Clinical and experimental Pharmacology and Physiology* **25**, 736–740.

43. **Gnaiger, E., Steinlechner-Maran, R., Méndez, G., Eberl, T. and Margreiter, R.,** (1995) Control of mitochondrial and cellular respiration by oxygen. *Journal of bioenergetics and biomembranes* 27, 583–596.
44. **Halliwell, B. and Gutteridge, J. M. C.** (2015) Free radicals in biology and medicine. *Oxford University Press.*
45. **Hampton, M., Nelson, B. T. and Andrews, M. T.** (2010). Circulation and metabolic rates in a natural hibernator: An integrative physiological model. *American Journal of Physiology-Regulatory, Integrative and Comparative Physiology* **299**, R1478–R1488.
46. **Hayward, L.** (2018) The effect of Anoxia on Mitochondrial Function in a Hibernator (Ictidomys tridecemlineatus) *Electronic thesis and Dissertation Repository*. 5880.
47. **Hillenius, W. J. and Ruben, J. A.** (2004). The Evolution of Endothermy in Terrestrial Vertebrates: Who? When? Why? *Physiological and Biochemical Zoology* **77**, 1019–1042.
48. **Hofer, A. and Wenz, T.** (2014). Post-translational modification of mitochondria as a novel mode of regulation. *Experimental Gerontology* **56**, 202–220.
49. **James, R. S., Staples, J. F., Brown, J. C. L., Tessier, S. N. and Storey, K. B.** (2013). The effects of hibernation on the contractile and biochemical properties of skeletal muscles in the thirteen-lined ground squirrel, Ictidomys tridecemlineatus. *Journal of Experimental Biology* **216**, 2587–2594.
50. **Jensen, B. S.** (2020). Hydrogen sulfide signaling: Interaction with hemeproteins and physiological effects. *Aarhus Universitet.*
51. **Kalogeris, T., Baines, C. P., Krenz, M. and Korthuis, R. J.** (2014) Cell Biology of Ischemia/Reperfusion Injury. *International review of cell and molecular biology.* **289**, 229–317.
52. **Kleinridders, A., Lauritzen, H. P. M. M., Ussar, S., Christensen, J. H., Mori, M. A., Bross, P. and Kahn, C. R.** (2013). Leptin regulation of Hsp60 impacts hypothalamic insulin signaling. *Journal of Clinical Investigation* **123**, 4667–4680.
53. **Kolomiytseva, I.K., Perepelkina, N.I. and Fesenko, E.E.** (2013). Lipids of liver membrane structures during hibernation of the Arctic ground squirrel Spermophilus undulatus. In *Doklady. Biochemistry and Biophysics*. **448**, 1–15.
54. **Kühlbrandt, W.** (2015) Structure and function of mitochondrial membrane protein complexes. *BMC Biology.* **13**, 1–11.
55. **Kurtz, C. C., Lindell, S. L., Mangino, M. J. and Carey, H. V.** (2006). Hibernation confers resistance to intestinal ischemia-reperfusion injury. *American Journal of Physiology-Liver Physiology* **291**, G895–G901.
56. **Lechler, E. and Penick, G. D.** (1963). Blood clotting defect in hibernating ground squirrels Citellus tridecemlineatus. *American Journal of Physiology* **5**, 985–988.
57. **Lee, Y. J. and Hallenbeck, J. M.** (2013) SUMO and Ischemic Tolerance. *Nuromoleculat medicine*. **15**, 771–781.
58. **Lee, J., Nam, J., Park, H.C., Na, G., Miura, K., Jin, J.B., Yoo, C.Y., Baek, D., Kim, D.H., Jeong, J.C. and Kim, D.** (2007). Salicylic acid-mediated innate immunity in Arabidopsis is regulated by SIZ1 SUMO E3 ligase. *The Plant Journal*, **49**, 79–90.

59. **Lehmer, E. M., Savage, L. T., Antolin, M. F. and Biggins, D. E.** (2006). Extreme Plasticity in Thermoregulatory Behaviors of Free-Ranging Black-Tailed Prairie Dogs. *Physiology and Biochemical Zoology.* **79**, 454–467.
60. **Lindell, S. L., Klahn, S. L., Piazza, T. M., Mangino, M. J., Torrealba, J. R., Southard, J. H. and Carey, H. V** (2005). Natural resistance to liver cold ischemia-reperfusion injury associated with the hibernation phenotype. *American Journal of Physiology-Gastrointestinal and Liver Physiology* **288**, 473–480.
61. **Lyman, C. P. and O'brien, R. C.** (1963). Autonomic control of circulation during the hibernation cycle in ground squirrels. *The Journal of Physiology*. **168**, 477.
62. **Maccannell, A. D. V, Jackson, E. C., Mathers, K. E. and Staples, J. F.** (2018). An improved method for detecting torpor entrance and arousal in a mammalian hibernator using heart rate data. *Journal of Experimental Biology*. **221**, 1–6.
63. **Maccannell, A. D. V, Sinclair, K. J., Mckenzie, C. A. and Staples, J. F.** (2019). Environmental temperature effects on adipose tissue growth in a hibernator. *Journal of Experimental Biology*. **222**, 1–8.
64. **Maccannell, A., Sinclair, K., Lannette Friesen-Waldner, ·, Charles, ·, Mckenzie, A. and Staples, J. F.** (2017). Water-fat MRI in a hibernator reveals seasonal growth of white and brown adipose tissue without cold exposure. *J Comparative Physiology B* **187**, 759–767.
65. **Mathers, K. E.** (2017) Regulation of liver mitochondrial metabolism during hibernation by post-translational modification. *Electronic Thesis and Dissertation Repository* 5098.
66. **Mathers, K. E., McFarlane, S. V., Zhao, L. and Staples, J. F.** (2017). Regulation of mitochondrial metabolism during hibernation by reversible suppression of electron transport system enzymes. *Journal of Comparative Physiology B* **187**, 227–234.
67. **Mathers, K. E. and Staples, J. F.** (2019). Differential posttranslational modification of mitochondrial enzymes corresponds with metabolic suppression during hibernation. *American Journal of Physiology and Integrative Comparative Physiology* **317**, R262–R269.
68. **McCarley, H.** (1966). Annual cycle, population dynamics and adaptive behavior of Citellus tridecemlineatus. *Journal of Mammalogy* **47**, 294–316.
69. **McFarlane, S. V, Mathers, K. E., Staples, J. F. and St, R.** (2017). Reversible temperature-dependent differences in brown adipose tissue respiration during torpor in a mammalian hibernator. *American Journal of Physiology and Integrative Comparative Physiology* **312**, 434–442.
70. **McNab, B. K.** (1974). The energetics of endotherms. *The Ohio Journal of Science*. **74**, 370–380.
71. **Miller, J.K., Brzezinska-Slebodzinska, E. and Madsen, F.C.** (1993) Oxidative stress, antioxidants, and animal function. *Journal of dairy science*, **76**, 812–2823.
72. **Muleme, H. M., Walpole, A. C. and Staples, J. F.** (2006) Mitochondrial Metabolism in Hibernation: Metabolic Suppression, Temperature Effects, and Substrate Preferences. *Physiology and Biochemical Zoology* **79** 474–483.

73. **Munro, D. and Treberg, J. R.** (2017). A radical shift in perspective: mitochondria as regulators of reactive oxygen species. *Journal of Experimental Biology* **220**, 1170–1180.
74. **Munro, D. and Thomas, D. W.** (2004). The role of polyunsaturated fatty acids in the expression of torpor by mammals: a review. *Zoology*. **107**, 29–49.
75. **Murphy, M. P.** (2016). Understanding and preventing mitochondrial oxidative damage. *Biochemical Society Transactions*. **44**, 1219–1226.
76. **Murry, C.E., Jennings, R.B. and Reimer, K.A.** (1986). Preconditioning with ischemia: a delay of lethal cell injury in ischemic myocardium. *Circulation*. **74**, 1124–1136.
77. **Nicholls, D.G. and Ferguson, S.J.** (2002). Bioenergetics. *Elsevier.*
78. **Nowell, M. M., Choi, H. and Rourke, B. C.** (2011). Muscle plasticity in hibernating ground squirrels (Spermophilus lateralis) is induced by seasonal, but not low-temperature, mechanism. *Journal of Comparative Physiology* **181**, 147–164.
79. **Nowack and Ruf** (2019). Always a price to pay: hibernation at low temperatures comes with a trade-off between energy savings and telomere damage. *Biology Letters* **15**, 20190466.
80. **Orr, A. L., Lohse, L. A., Drew, K. L. and Hermes-Lima, M.** (2009). Physiological oxidative stress after arousal from hibernation in Arctic ground squirrel. *Comparative Biochemistry and Physiology. - A Molecular Integrative Physiology* **153**, 213–221.
81. **Otis, J. P., Pike, A. C., Torrealba, J. R., Hannah, · and Carey, V.** (2017). Hibernation reduces cellular damage caused by warm hepatic ischemia-reperfusion in ground squirrels. *Journal of Comparative Physiology B* **187**, 639–648.
82. **Ou, J.**, **Ball, J. M., Laun, Y., Zhao, T., Miyagishima, K. J., Xu, Y., Zhou, H., Chen, J., Merriman, D. K., Xie, Z., Mallon, B.S., Li, W.** (2018) iPSCs from a hibernator provide a platform for studying cold adaption and its potential medical applications. *Cell* **173**, 851–863.
83. **Page, M. M., Peters, C. W., Staples, J. F. and Stuart, J. A.** (2008). Intracellular antioxidant enzymes are not globally upregulated during hibernation in the major oxidative tissues of the 13-lined ground squirrel Spermophilus tridecemlineatus. *Comparative Biochemistry and Physiology - A Molecular Integrative Physiology* **152**, 115–122.
84. **Park, S.-Y., Gifford, J. R., Andtbacka, R. H. I., Trinity, J. D., Hyngstrom, J. R., Garten, R. S., Diakos, N. A., Ives, S. J., Dela, F., Larsen, S., et al.** (2014). Cardiac, skeletal, and smooth muscle mitochondrial respiration: are all mitochondria created equal? *American Journal of Physiology-Heart and Circulatory Physiology* **307**, 346–352.
85. **Paradies, G., Paradies, V., De Benedictis, V., Ruggiero, F.M. and Petrosillo, G.** (2014). Functional role of cardiolipin in mitochondrial bioenergetics. *Biochimica et Biophysica Acta (BBA)-Bioenergetics*, **1837**, 408–417.

86. **Pengelley, E. T. and Fisher, C.** (1961). Rhythmical arousal from hibernation in the golden-mantled ground squirrel, Citellus lateralis tescorum. *Canadian Journal of Zoology* **39**, 105–120.
87. **Revsbech, I.G., Shen, X., Chakravarti, R., Jensen, F.B., Thiel, B., Evans, A.L., Kindberg, J., Fröbert, O., Stuehr, D.J., Kevil, C.G. and Fago, A.** (2014). Hydrogen sulfide and nitric oxide metabolites in the blood of free-ranging brown bears and their potential roles in hibernation. *Free Radical Biology and Medicine*. **73,** 349–357.
88. **Robb, E. L., Hall, A. R., Prime, T. A., Eaton, S., Szibor, M., Viscomi, C., James, A. M., Michael, X. and Murphy, P.** (2018). Control of mitochondrial superoxide production by reverse electron transport at complex I. *Biological Chemistry*. **293**, 9869–9879.
89. **Rouble, A. N., Tessier, S. N. and Storey, K. B.** (2014) Characterization of adipocyte stress response pathways during hibernation in thirteen-lined ground squirrels. *Molecular and Cellular Biochemistry* **393**, 271–282.
90. **Ruf, T. and Geiser, F.** (2015). Daily torpor and hibernation in birds and mammals. *Biology Review* **90**, 891–926.
91. **Russel, R. L., O'Neill, P. H., Epperson, L.E., Martin, S. L.** (2010). Extensive use of torpor in 13-lined ground squirrels in the fall prior to cold exposure. *Journal of Comparative Physiology B* **180**, 1165–1172.
92. **Scheck, S. H. and Fleharty, E. D.** (1979) Daily energy budgets and patterns of activity of the adult thirteen-lined ground squirrel, Spermophilus tridecemlineatus. *Physiological Zoology* **52**, 390–397.
93. **Sekijima, T., Ishiniwa, H. and Kondo, N.** (2012). Phylogenetic Background of Hibernation and Hibernation-Specific Proteins in Sciuridae. In *Living in a Seasonal World*, 327–335.
94. **Serkova, N.J., Rose, J.C., Epperson, L.E., Carey, H.V. and Martin, S.L**. (2007) Quantitative analysis of liver metabolites in three stages of the circannual hibernation cycle in 13-lined ground squirrels by NMR. *Physiological genomics*, **31**, 15–24.
95. **Smit, B. and McKechnie, A. E.** (2010). Avian seasonal metabolic variation in a subtropical desert: basal metabolic rates are lower in winter than in summer. *Functional Ecology* **24**, 330–339.
96. **Snapp, B. D. and Heller, H. C.** (1981). Suppression of metabolism during hibernation in ground squirrels (citellus lateralis). *Physiological Zoology.* **54**, 297–307.
97. **Sokol, R. J., Dwereaux, M. and Khandwala, R. A.** (1991) Effect of dietary lipid and vitamin E on mitochondrial lipid peroxidation and hepatic injury in the bile duct-ligated rat'. *Journal of lipid research.* **32**, 1349–1357.
98. **Sparling, C.E. and Fedak, M.A.** (2004) Metabolic rates of captive grey seals during voluntary diving. *Journal of Experimental Biology* **207**, 1615–1624.
99. **Staples, J. F.** (2016). Metabolic Flexibility: Hibernation, Torpor, and Estivation. Metabolic Flexibility: Hibernation, Torpor, and Estivation. *Comparative Physiology* **6**, 737–771.

100. **Staples, J. F. and Brown, J. C. L.** (2008). Mitochondrial metabolism in hibernation and daily torpor: A review. *Journal of Comparative Physiology B* **178**, 811–827.
101. **Staples, J. F. and Mathers K.** (2018).
102. **Storey, K. B.** (2010). Out could: biochemical regulation of mammalian hibernation-a mini-review. *Gerontology* **56**, 220–230.
103. **Tøien, Ø., Drew, K. L., Chao, M. L. and Rice, M. E.** (2001). Ascorbate dynamics and oxygen consumption during arousal from hibernation in Arctic ground squirrels. *American Journal of Physiology-Regulatory* **281**, R572–R583.
104. **Vaughan, D. K., Gruber, A. R., Michalski, M. L., Seidling, J. and Schlink, S.** (2006). Capture, care, and captive breeding of 13-lined ground squirrels, Spermophilus tridecemlineatus. *Laboratory Animal (NY).* **35**, 33–40.
105. **Wade, O.** (1930). The behaviour of certain spermiphiles with special reference to aestivation of hibernation. *Journal of Mammology* **11**, 160–188.
106. **Walters, A.M., Porter, G.A. and Brookes, P.S.** (2012) Mitochondria as a drug target in ischemia heart disease and cardiomyopathy. *Circulation Research* **111**, 1222–1236.
107. **Wang, L. C., McArthur, M., Jourdan, M.L. and Lee, T.F.** (1990) Depressed metabolic rate in hibernation and hypothermia: can these be compared meaningfully? *Hypoxia: the adaptions.* 78–83.
108. **Wei, Y., Zhang, J., Xu, S., Peng, X., Yan, X., Li, X., Wang, H., Chang, H. and Gao, Y.** (2018) Controllable oxidative stress and tissue specificity in major tissues during the torpor-arousal cycle in hibernating Daurian ground squirrels. *Royal Society Open Biology*. **8**, 1–14.
109. **Woods, C. P., Zenon, ·, Czenze, J. and Brigham, · R Mark** (2019). The avian "hibernation" enigma: thermoregulatory patterns and roost choice of the common poorwill. *Oecologia* **1**, 47–53.
110. **Wickler, S. J. and Hoyt, D. F.** (1991). Disuse atrophy in the hibernating golden-mantled ground squirrel, Spermophilus lateralis. *American Journal of Physiology-Regulatory, Integrative and Comparative Physiology* **261**, R1212–R1217.
111. **Zweier, J. L. Flatherty, J. T. and Weisfeldt, M. L.** (1987) Direct measurement of free radical generation following reperfusion of ischemia myocardium. *Proceedings of the National Academy of Sciences.* **84**, 1404–1407.

Appendix

Appendix 1: Animal use ethics approval

Western

2012-016:5:

AUP Number: 2012-016
AUP Title: Regulation of mitochondrial metabolism in mammalian hibernation and ageing.
Yearly Renewal Date: 08/05/2016

The YEARLY RENEWAL to Animal Use Protocol (AUP) 2012-016 has been approved by the Animal Care Committee (ACC), and will be approved for one year following the above review date.

Please at this time review your AUP with your research team to ensure full understanding by everyone listed within this AUP.

As per your declaration within this approved AUP, you are obligated to ensure that:

1) Animals used in this research project will be cared for in alignment with:
   a) Western's Senate MAPPs 7.12, 7.10, and 7.15
   http://www.uwo.ca/univsec/policies_procedures/research.html
   b) University Council on Animal Care Policies and related Animal Care Committee procedures
   http://uwo.ca/research/services/animalethics/animal_care_and_use_policies.html
2) As per UCAC's Animal Use Protocols Policy,
   a) this AUP accurately represents intended animal use;
   b) external approvals associated with this AUP, including permits and scientific/departmental peer approvals, are complete and accurate;
   c) any divergence from this AUP will not be undertaken until the related Protocol Modification is approved by the ACC; and
   d) AUP form submissions - Annual Protocol Renewals and Full AUP Renewals - will be submitted and attended to within timeframes outlined by the ACC. http://uwo.ca/research/services/animalethics/animal_use_protocols.html
3) As per MAPP 7.10 all individuals listed within this AUP as having any hands-on animal contact will
   a) be made familiar with and have direct access to this AUP;
   b) complete all required CCAC mandatory training (_training@uwo.ca); and
   c) be overseen by me to ensure appropriate care and use of animals.
4) As per MAPP 7.15,
   a) Practice will align with approved AUP elements;
   b) Unrestricted access to all animal areas will be given to ACVS Veterinarians and ACC Leaders;
   c) UCAC policies and related ACC procedures will be followed, including but not limited to:
      i) Research Animal Procurement
      ii) Animal Care and Use Records
      iii) Sick Animal Response
      iv) Continuing Care Visits
5) As per institutional OH&S policies, all individuals listed within this AUP who will be using or potentially exposed to hazardous materials will have completed in advance the appropriate institutional OH&S training, facility-level training, and reviewed related (M)SDS Sheets, http://www.uwo.ca/hr/learning/required/index.html

Submitted by: Copeman, Laura
on behalf of the Animal Care Committee
University Council on Animal Care

Appendix 2:

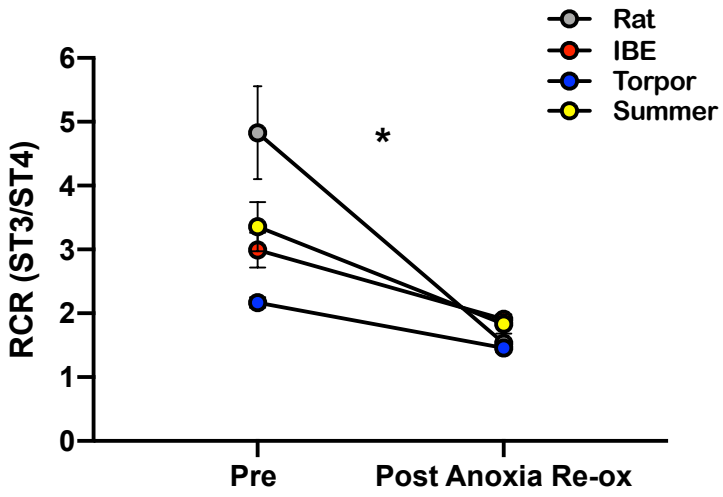

Interaction plot of the respiratory control ratio (RCR) of liver mitochondria before (pre) and post anoxia-reoxygenation. Data are presented as mean ± SE for N_{Rat}=4, N_{IBE}=14, N_T=17, N_S=8. Demonstrating healthy rat mitochondria before anoxia-reoxygenation despite delayed sampling time post-mortem. Anoxia-reoxygenation significantly decreased RCR in all groups (*, P_{Rat}=0.012; P_{IBE}<0.001; P_T<0.0001; P_S=0.001, paired two-sided t-test).

Curriculum Vitae

Name: Brynne Duffy

Post-secondary Education and Degrees:
The University of Western Ontario
London, Ontario, Canada
2020 M.Sc.

The University of Western Ontario
London, Ontario, Canada
2013-2018 B.Sc.

Awards
Spring 2020 travel award, Western University Biology Graduate Education Committee.

Best student poster, International conference of comparative physiology and biochemistry 2019.

Runner-up student poster, International conference of comparative physiology and biochemistry 2019.

Presentations:

Duffy, B. & Staples, J.F. (2020) Reactive oxygen species damage and functional consequences in the hibernating 13-lined ground squirrel. 29th annual comparative physiology and biochemistry workshop, Rice Lake, Keene, ON, Canada. [Oral]

Duffy, B. & Staples, J.F. (2019) Reactive oxygen species damage and functional consequences in different hibernation states of the thirteen lined ground squirrel. Biology graduate research forum, London, ON, Canada. [Oral]

Duffy, B., Jensen, B.J. & Staples, J.F. (2019) Reactive oxygen species damage and functional consequences in different hibernation states of the thirteen lined ground squirrel. International congress of comparative physiology and biochemistry, Ottawa, ON, Canada. [Poster]

Duffy, B. & Staples, J.F. (2019) Reactive oxygen species damage and functional consequences in the hibernating 13-lined ground squirrel. Vox Talk, McMaster University, Hamilton, ON, Canada. [Invited speaker]

Jensen, B., Duffy, B., Kevil, C.G., Fago, A., Staples, J. (2019) Does hydrogen sulfide metabolism differ among hibernation states in 13-lined ground squirrels? International congress of comparative physiology and biochemistry, Ottawa, ON, Canada [Oral]